ORNL-5581

Tritium Separation From Light and Heavy Water by Bipolar Electrolysis

D. W. Ramey
M. Petek
R. D. Taylor
E. H. Kobisk
J. Ramey
C. A. Sampson

OAK RIDGE NATIONAL LABORATORY
OPERATED BY UNION CARBIDE CORPORATION · FOR THE DEPARTMENT OF ENERGY

ORNL-5581
Dist. Category
UC-70

Contract No. W-7405-eng-26

Solid State Division

NUCLEAR FUEL AND WASTE PROGRAMS

NATIONAL AIRBORNE WASTE PROGRAM

TRITIUM SEPARATION FROM LIGHT AND HEAVY WATER BY BIPOLAR ELECTROLYSIS

D. W. Ramey, M Petek, R. D. Taylor, E. H. Kobisk, J. Ramey, C. A. Sampson

MASTER

Date Published: October 1979

OAK RIDGE NATIONAL LABORATORY
Oak Ridge, Tennessee 37830
operated by
UNION CARBIDE CORPORATION
for the
DEPARTMENT OF ENERGY

CONTENTS

BLANK PAGE

LIST OF TABLES

LIST OF FIGURES

BLANK PAGE

LIST OF FIGURES (contd)

LIST OF FIGURES (contd)

LIST OF FIGURES (contd)

TRITIUM SEPARATION FROM LIGHT AND HEAVY WATER BY BIPOLAR ELECTROLYSIS

D. W. Ramey, M. Petek, R. Taylor, E. H. Kobisk, J. Ramey, C. Sampson

ABSTRACT

Use of bipolar electrolysis with countercurrent electrolyte flow to separate hydrogen isotopes was experimentally and theoretically investigated to develop a process for the removal of tritium from light water effluents from nuclear installations or from the heavy water moderator in nuclear reactors. Possible application of this technology to the separation of deuterium from natural light water also seems feasible. Deuterium-tritium and protium-tritium separation factors occurring on a Pd-25% Ag bipolar electrode were measured to be 2.05-2.16 and 11.6-12.4 respectively, at current densities between 0.21-0.50 A cm^{-2}, and at 35-90°C. Current densities up to 0.3 A cm^{-2} have been achieved in continuous operation, at 80-90°C, without significant gas formation on the bipolar electrodes. From the measured overvoltage at the bipolar electrodes and the electrolyte conductivity the power consumption per stage was calculated to be 3.0 kwh/kg H_2O at 0.2 A cm^{-2} and 5.0 kwh/kg H_2O at 0.5 A cm^{-2} current density, compared to 6.4 and 8.0 kwh/kg H_2O for normal electrolysis, at the respective current densities. A mathematical model for hydrogen isotope separation by bipolar electrolysis, i.e., for a square cascade, was derived and proven to accurately describe the results for protium-tritium separation in two laboratory scale, multistage

experiments with countercurrent electrolyte flow; the measured tritium concentration gradient through the cascade agreed with the calculated values.

Generally, bipolar electrolytic separation of tritium appears feasible, however, further research, development, and engineering studies are required. This report contains discussions of pertinent literature and experimental data involving electrode materials, bipolar cell design, bipolar electrolytic cell operations, power requirements, separation factors, electrolyte maintenance, and mathematical theory.

INTRODUCTION

Tritium production is a natural consequence of fission or of neutron breeding in light or heavy water reactor moderators. Removal of this radioisotope to avoid discharge to the environment and/or to minimize personnel exposure and ingestion are problems of a continuing and increasing nature. The purpose of this work is to develop a method suitable for continuous removal of tritium from aqueous effluents arising from the above noted sources. The appropriate tritium removal process must be capable of treating very large volumes of water having low tritium content. Furthermore, the separative process equipment must be as small as practicable to keep containment cost to a minimum. The approach taken in this work is to remove tritium from contaminated light and heavy water by an electrolytic process known as bipolar electrolysis (BPE). With the appropriate variations in the process design, BPE also may be

applied to heavy water production and possibly to the effluents from reactor fuel reprocessing.

It is the character of the bipolar electrolytic process that multiple separation of hydrogen isotopes can be realized within a single electrolysis cell without the formation of gases, except at the terminal anode and cathode. This unique characteristic offers a much simplified material flow between separation stages as compared to conventional electrolysis, where gaseous products evolve from every separation stage and subsequently must be converted to water before entering the adjacent stages. An additional major advantage of the bipolar process is its potential ability to consume less power than conventional electrolysis having equivalent separative capability.

Application of countercurrent electrolysis using hydrogen-permeable bipolar electrodes to separate hydrogen isotopes was proposed by Salmon in 1956 (1) and some aspects of the proposed process were discussed by Barr and Drews (2) in 1960 for its application to heavy water production. Drazic (3) and Ribnikar and Pupezin (4) suggested the method as a potential process for the removal of tritium from reactor coolant or other contaminated effluents. In the proposed process, bipolar electrodes are placed between two terminal electrodes in an electrolytic cell (see Figure 1). The bipolar electrodes are fabricated from a material that is impermeable to the electrolyte but can be permeated by elemental hydrogen. Hydrogen produced at the cathodic surface of the bipolar electrodes, diffuses through the electrode material to the anodic surface where

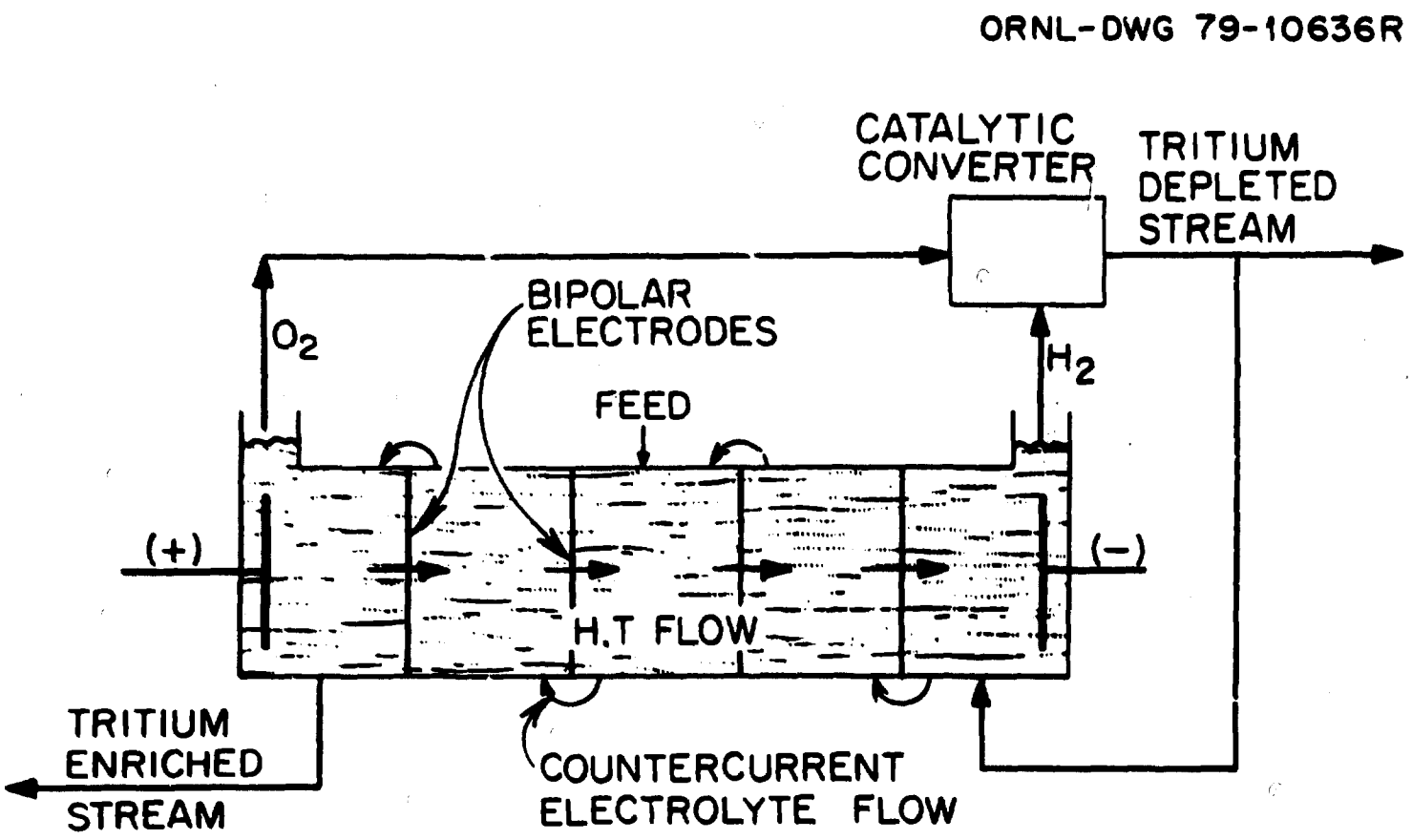

Figure 1. Schematic representation of the bipolar electrolysis cell with countercurrent electrolyte flow.

it is oxidized to water. Flow of hydrogen is established through the system from the terminal anode toward the terminal cathode, with gaseous hydrogen evolving only at the terminal cathode. The mechanism of hydrogen transport through the bipolar electrode consists of several processes: electro-reduction at the cathodic surface, permeation through the electrode, and electro-oxidation at the anodic surface. All three processes occur more rapidly for the lighter isotope, thus enrichment of the heavy isotope occurs in the electrolyte adjacent to the cathodic surface of each bipolar electrode and the net flow of tritium is towards the anode compartment. Electrolyte feed solution is added to the system continuously and the electrolyte is circulated countercurrent to the hydrogen mass flow from one compartment to the next; this results in a cascade system from which tritium-rich and tritium-poor streams can be withdrawn from opposite ends of the cell.

To operate such a system continuously in an efficient manner, several conditions must be fulfilled:

1. The electrode material must be sufficiently permeable to hydrogen so that an appreciable current density can be applied without forming gaseous products (O_2 and H_2). This condition is necessary to minimize the cost of the electrodes and to achieve a compact cell design. This latter constraint of cell size is important to minimize the containment cost that will be incurred when the tritium content is enriched to a high level (>200 Ci/liter).

2. Power losses, and hence the voltage drop across the individual compartments, must be comparable or less than that of conventional electrolysis so as to keep the process economically feasible.
3. Separation factors for protium-tritium and deuterium-tritium must be known so that cascade design may be optimized for maximum throughput.
4. The parameters governing the efficiency of separation of hydrogen isotopes throughout the cascade require definition so that desired enrichment (or depletion) can be achieved with minimum power consumption.
5. A continuous electrolyte maintenance system is necessary to assure a functionally constant electrolyte concentration throughout the cascade.
6. A variety of analytical techniques require development to determine the isotope distribution throughout the cascade.

In this report, the existing knowledge of the bipolar tritium separation process will be discussed along with the results obtained in studies of electrode material, power consumption in the bipolar process, separation factor per stage, cascade design, and electrolyte maintenance. For each of these topics the present state of knowledge will be presented, our experimental results summarized, and appropriate future research activities suggested. General conclusions are presented in the summary. More detailed descriptions of specific problems are presented in Appendices.

ELECTRODE MATERIAL

Introduction

The capacity of palladium to dissolve hydrogen, its remarkable resistance to chemical attack, and its ductility (that permits it to be rolled into very thin, pinhole free foils >0.0025 cm) makes palladium a prime candidate for use as a bipolar electrode. The solubility, diffusion, and nature of dissolved hydrogen in palladium have been studied both by gas-solid phase experiments as well as by using in situ electrolytically generated hydrogen. An extensive review of the palladium-hydrogen system is given in the monograph by Lewis (5).

Unless the metal surface has been suitably activiated (6-8), the rate-controlling step in the hydrogen permeation process is its adsorption from the gaseous phase, or if produced electrolytically, from the metal surface into the bulk of the metal. For activated palladium membranes, the rate of diffusion and solubility of hydrogen become the permeation rate-determining factors (8-11).

At temperatures between 20 and 100°C (at 1 atm H_2), which are of interest in the electrolytic production of hydrogen from aqueous solutions, there are two phases of palladium-hydrogen: the low hydrogen content α-phase with maximum H/Pd atomic ratio of 0.015 and the hydrogen-rich β-phase with H/Pd ratio of 0.7 at room temperature and 1 atm H_2 (5, 12, 13). Transition from the α-phase to the β-phase is accompanied by an increase in crystal lattice volume, and, consequently, repeated solution

and desorption of hydrogen leads to mechanical deterioration of the material (12). Such behavior is detrimental to long-term BPE application requiring mechanical stability.

Problems associated with the phase transition can be avoided by using a palladium-silver alloy containing 25-30% silver, for which only one palladium-silver-hydrogen phase exists at temperatures 20-100°C (5, 12, 15, 16). Deformation of the alloy lattice caused by sorption-desorption of hydrogen is considerably smaller as compared to pure palladium deformation; the alloy material remains mechanically stable over a prolonged period.

There is, however, a lower solubility of hydrogen in palladium-silver: 0.52 H/Pd at 25°C and 1 Atm H_2 for Pd-25% Ag, compared to 0.7 H/Pd for pure palladium under the same conditions (16), and a somewhat lower diffusion coefficient: $D_{Pd-25\% Ag} = 3 \times 10^{-7}$ cm^2 sec^{-1} (17) or 7.3×10^{-7} (18) as compared to $D_\beta = 1.4 \times 10^{-6}$ (6) at 25°C. The maximum current density, i, achieviable for a Pd-25% Ag membrane can be calculated from Fick's first Law:

$$\frac{dN}{q\ dt} = \frac{i}{nF} = D_{Pd/Ag}\ \frac{dC}{dx}\ , \qquad (1)$$

where N = number of moles of H_2, t = time, q = cross sectional area, n = number of electrons exchanged in the electrode reaction, F = faraday, D = diffusion coefficient, dC = concentration gradient through the membrane and dx is the membrane thickness.

From the diffusion coefficient and solubility of hydrogen in Pd-25% Ag, Kussner (17) calculated the m.c.d.* to be 0.120 A cm^{-2}, for a 0.01 cm thick anode having one side exposed to the electrolyte and the other to hydrogen gas at 1 atm pressure and 20°C. Von Stackelberg and Ludwig (10) imposed a constant current through the cathodic interface of a bipolar electrode, keeping the anodic interface at such a potential that the only electrode reaction was the oxidation of the hydrogen diffusing through the palladium. In these experiments 91-97% recovery of hydrogen at the anodic surface was achieved at current densities between 0.060 and 0.270 A cm^{-2} on 0.0104 cm thick palladium electrodes activated by surface oxidation. Palladium-silver alloy electrodes were not studied by Von Stackelberg and Ludwig.

In an attempt to avoid the high cost of palladium, Drazic fabricated hydrophobic, porous, catalyst-impregnated carbon electrodes for use as bipolar electrodes for hydrogen isotope separation (3). This limited research effort resulted in a m.c.d. of 0.07 A cm^{-2}.

Experimental Results and Discussion

Selection of the Bipolar Electrode Material. In the early stages of research on the bipolar process as performed at ORNL, an attempt was made

---

*The term "maximum current density" - m.c.d. - will be used hereafter for a current density slightly below the current density at which gas bubbles appear at the bipolar electrode surfaces.

to use hydrophobic, porous carbon electrodes produced by a method similar to that reported by Drazic (3). Although the electrodes appeared to be sufficiently hydrophobic and a value of 0.07 A cm^{-2} m.c.d. could be achieved, the anodic surfaces experienced oxidative degradation and failed mechanically. Further research using carbon electrodes was abandoned. The high current densities achievable with Pd and Pd-Ag alloys, as noted above, indicated that these materials, although more expensive, could be economically used for the bipolar process. Application of very thin foils at high current densities could lead to a very compact and efficient cascade cell design.

Since continuous cell operation does not require repetitive charging and removal of hydrogen from the bipolar electrodes, pure palladium was tested initially as the electrode material. Palladium foils, 0.0025-0.0076 cm thick, were cleaned and annealed at 700°C in a hydrogen atmosphere for one hour. To establish an initial hydrogen concentration in the bipolar electrode, each palladium electrode was connected temporarily as a cathode, while one of the terminal electrodes of the cell served as the anode (see Figure 2). The electrode was charged with 0.05 A cm^{-2} until the generation of gas bubbles on both sides of the electrode indicated saturation of the palladium with hydrogen. Hydrogen impregnation was then discontinued, and then only the terminal cathode and anode were connected to the power source. Current densities up to 0.07 A cm^{-2} could be passed without bubble formation at the bipolar electrode. After operation for several days however, the palladium foil became distorted and peripheral areas were severely wrinkled where a mechanical seal had been applied to the electrode. The apparent cause for the

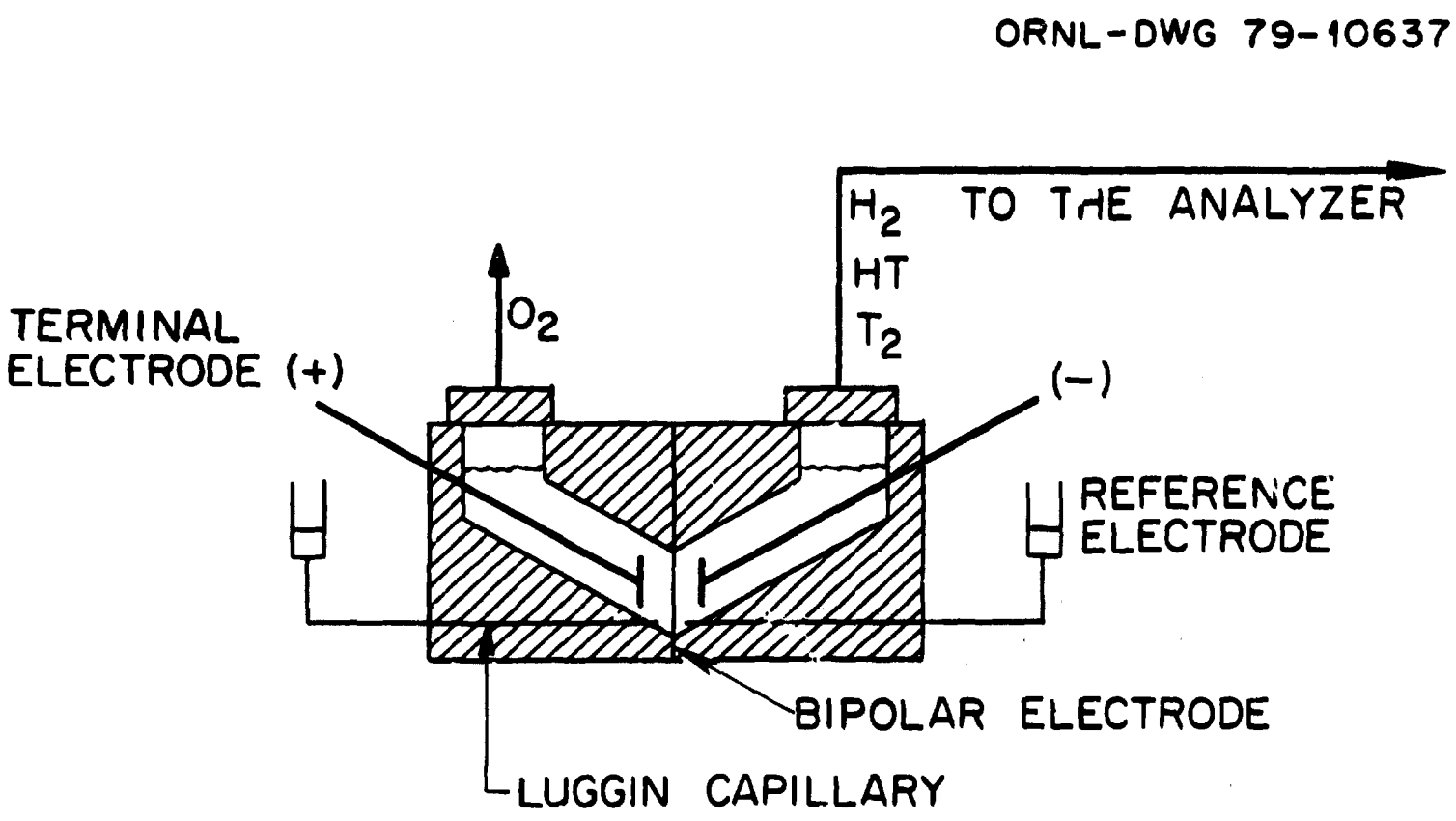

Figure 2. Single bipolar electrolysis cell.

material distortion was non-uniform distribution of hydrogen within the electrode material.

Palladium - 25% silver alloy electrodes exhibited considerably less distortion than those of pure palladium. This alloy material is available from Matthey-Bishop, Inc. in pinhole-free foils as thin as 0.0038 cm and 11.43-cm wide strips up to 122 m long. Using this material, differences in composition or in the manufacturing process could be excluded as possible causes for variations in the electrode behavior. Considering properties of Pd-25% Ag alloy and its commercial availability, this material was selected for further experiments in studying the feasibility of the hydrogen isotope separation process.

Surface Activation. When the Pd-Ag foils were pretreated in the same manner as was described for the Pd foils, the m.c.d. was 0.07 A cm^{-2} at 30°C. To increase this throughput, several surface activation procedures were tested. Palladizing both surfaces of the electrode caused hydrogen bubble formation at even lower current densities than that for non-palladized electrodes. Electron micrographs of the palladized surfaces showed a dense coverage of sharp, spiny crystallites (Fig. 3). It was speculated that local super-saturation of hydrogen could occur at the points, causing bubble formation at low current densities. Therefore, the palladized electrode was passed through steel rollers to flatten the sharp edges of the crystallites, yet retaining the rough surface. After this treatment hydrogen throughput was somewhat improved, but not in excess of . cm^{-2}. Sputter-etching, followed by redeposition of a thin layer of palladium on a Pd-25% Ag electrode caused profuse hydrogen bubble evolution to occur at low current densities (<0.07 A cm^{-2}).

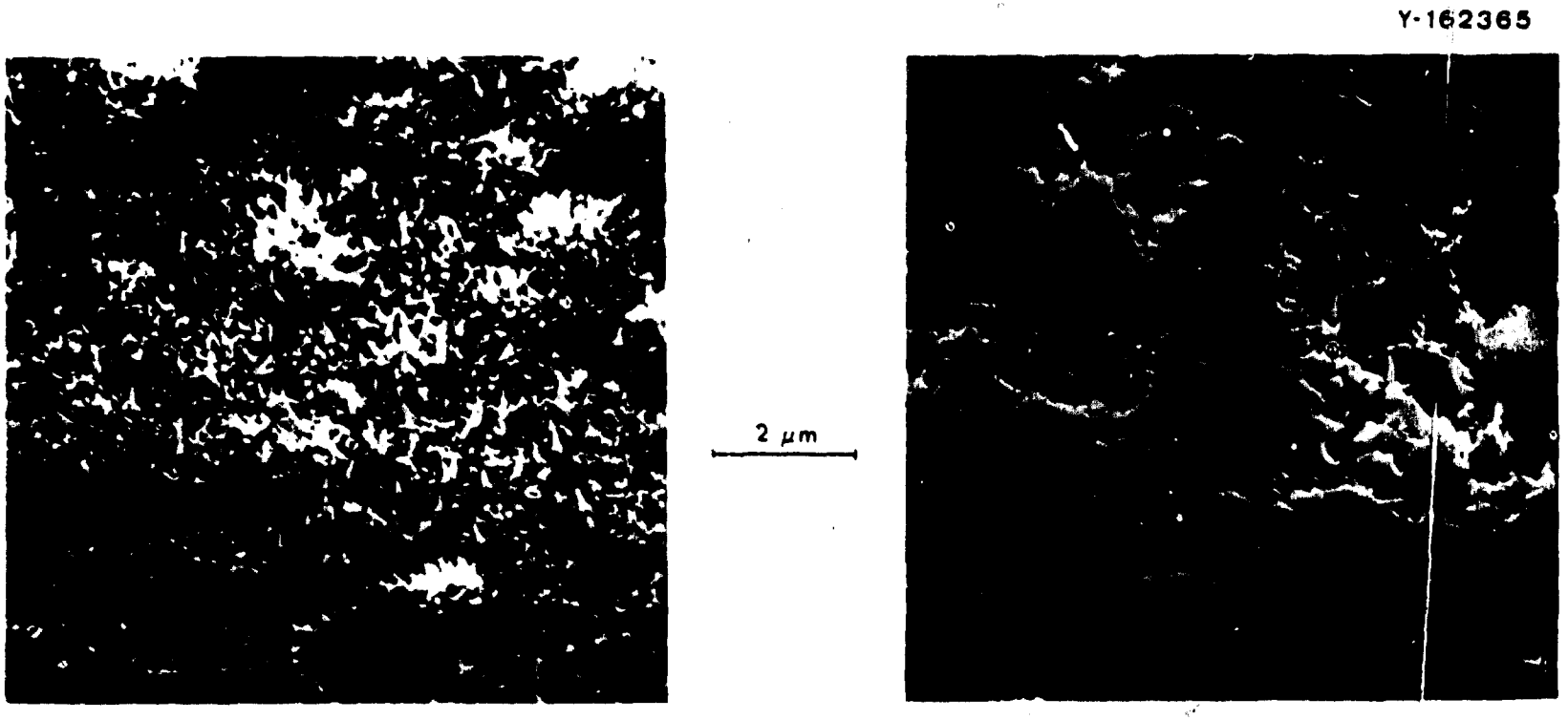

Figure 3. a. Electron micrograph of a Pd-25% Ag foil after palladizing. 10 K enlargement.

b. The same foil after rolling. 10 K enlargement.

The surface activation method suggested by Serfass (19) was found to be a suitable procedure. After rigorous cleaning with detergent, followed by rinsing with distilled water, acetone and CCl_4, the electrode material was annealed at 700°C for one hour in a H_2 atmosphere. After preheating the electrode to 200°C in air, subsequent dipping for 5 sec. in molten NaOH at 700°C caused the bright metal surfaces to turn brownish-black. An electron micrograph of the electrode showed the surface to be etched, highlighting crystalline microfacets (Fig. 4). Electrodes treated in this manner were found to operate at high current densities over continuous periods of three weeks or more without loss of their enhanced protium and deuterium permeability.

The maximum current density achievable can be calculated, assuming that the protium concentration at the cathode surface approaches saturation and at the anode surface approaches zero. Using the solubility data of protium in Pd-Ag alloys as reported by Brodowsky and Poeschel (16), and the diffusion coefficient for protium in Pd-25% Ag at temperatures from 0-90°C, as reported by Kussner (17) and Wicke and Holleck (18), the saturation concentration of protium was calculated using Equation (1) for various membrane thicknesses (see Figure 5). Details of these calculations are given in Appendix A. In the same manner the m.c.d. for the D_2O-Pd-25% Ag-D_2 system may be calculated. However, neither the solubility data for deuterium in the Pd-25% Ag alloy nor its diffusion coefficients in the 25-100°C temperature range are readily available. By analogy with the palladium-deuterium and palladium-protium

Y-162366

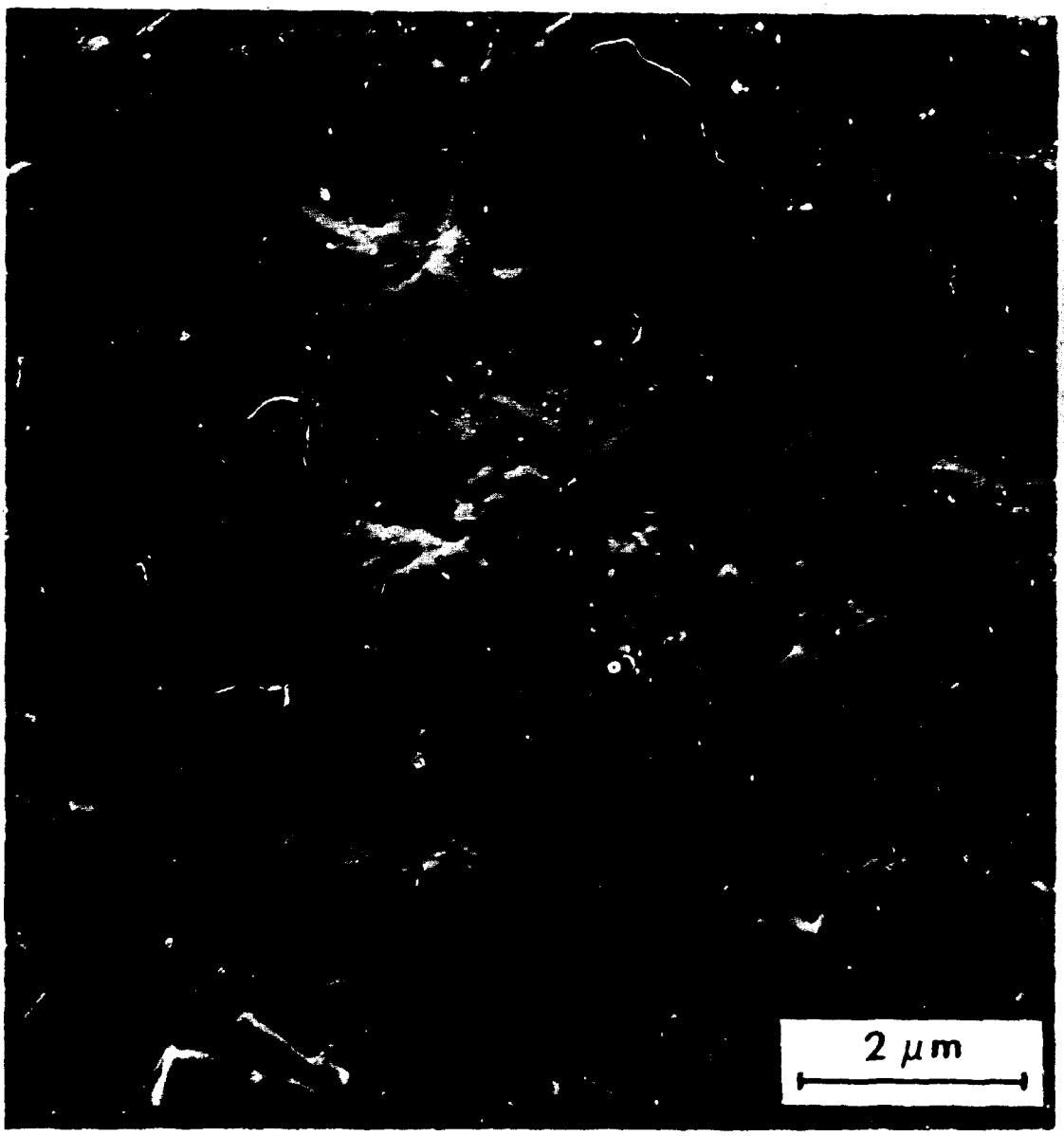

Pd-25% Ag FOIL AFTER EXPOSURE TO MOLTEN NaOH

Figure 4. Electron micrograph of Pd-25% Ag foil activated by dipping into molten NaOH.

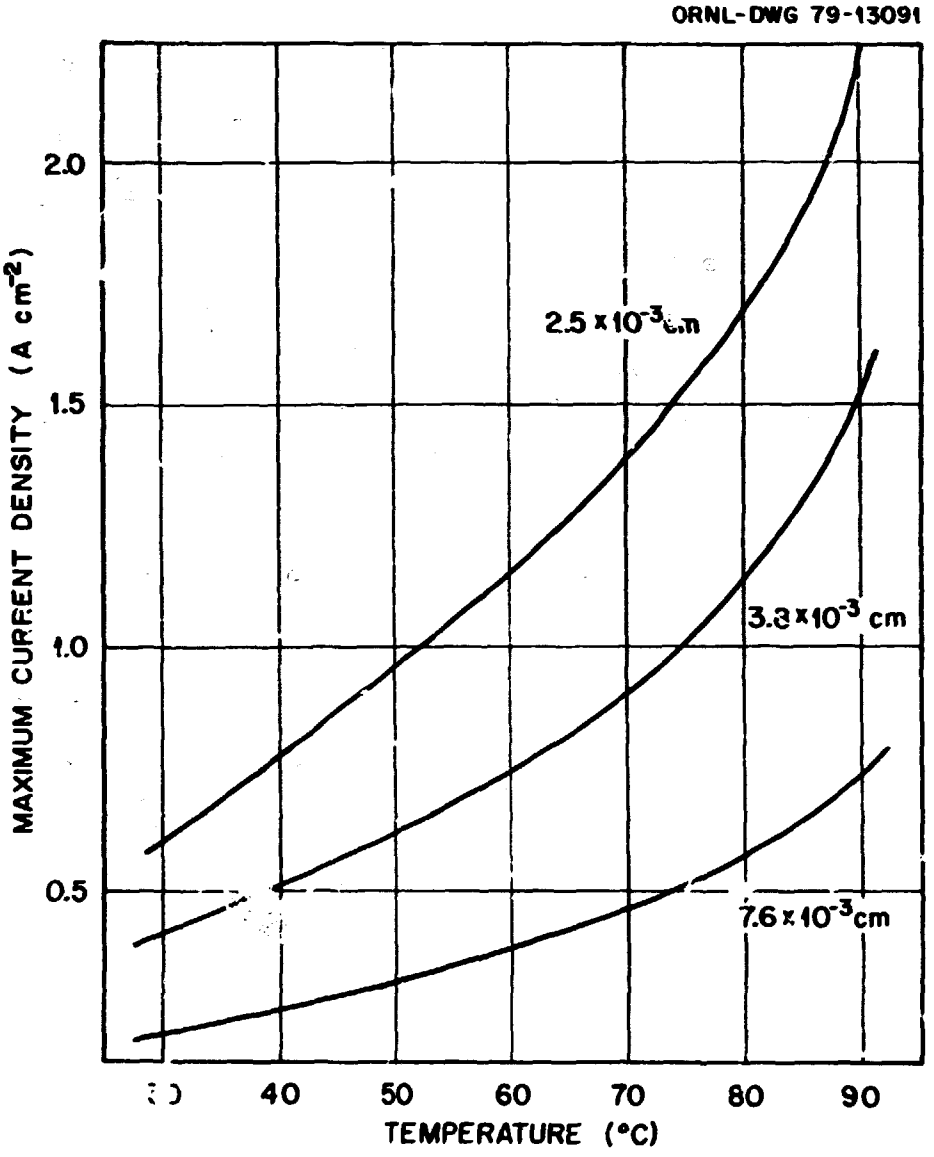

Figure 5. Maximum current density calculated for a 2.5 x 10^{-3}, 3.8 x 10^{-3} and 7.6 x 10^{-3} cm thick Pd-25% Ag foil.

systems*, the solubility of deuterium would be expected to be less than that of protium. This would imply that a smaller m.c.d. would be observed in the D_2O system. However, some compensation may be realized by the fact that, according to some reports (5), deuterium diffuses through palladium faster than protium (although there is a seeming conflict in the literature on this point).

A small thermostated cell, similar to that shown in Fig. 2, was used to study the voltage drop across the bipolar electrode and to determine the m.c.d. under various conditions. Palladium–hydrogen reference electrodes were used to monitor the anodic and the cathodic potential of the bipolar electrode as a function of current density, temperature, electrode thickness, and the electrolyte composition. Voltage measurements were taken after a 30-min. stabilization period at a specific current density. Either 3 N or 6 N NaOH was used for the electrolyte. No effect of NaOH concentration on the anodic or cathodic potentials of the electrode was found. Within the entire temperature range studied (40-90°C) the 2.5×10^{-3} cm thick electrodes remained completely permeable to hydrogen even at a current density of 0.4 A cm^{-2} (see Fig. 6). At the same current density with a 7.6×10^{-3} cm thick bipolar electrode, gas bubble formation was observed at temperatures below 60°C, which ceased when the temperature was increased above this value. It was observed that gas formation at the anode surface was associated with a considerable increase in anode potential whereas the cathode surface potential

---

*The saturation concentration of protium at 1 atm. and 80°C is H/Pd = 0.63 compared to D/Pd = 0.52 for deuterium under the same conditions.

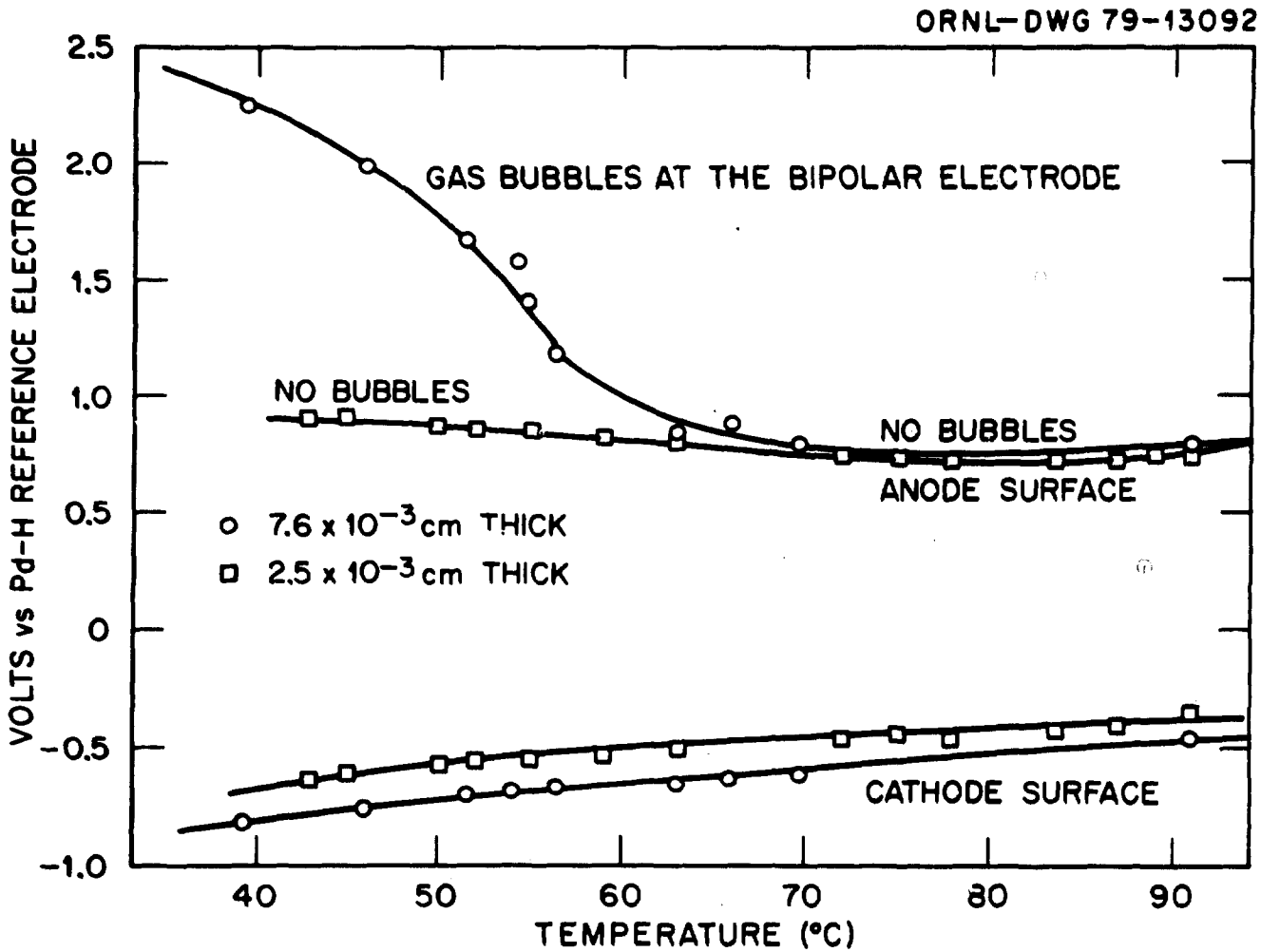

Figure 6. Temperature dependence of the anodic and the cathodic surface potential of the bipolar electrode at 0.4 A cm^{-2} current density. Electrolyte: 6 N NaOH in H_2O.

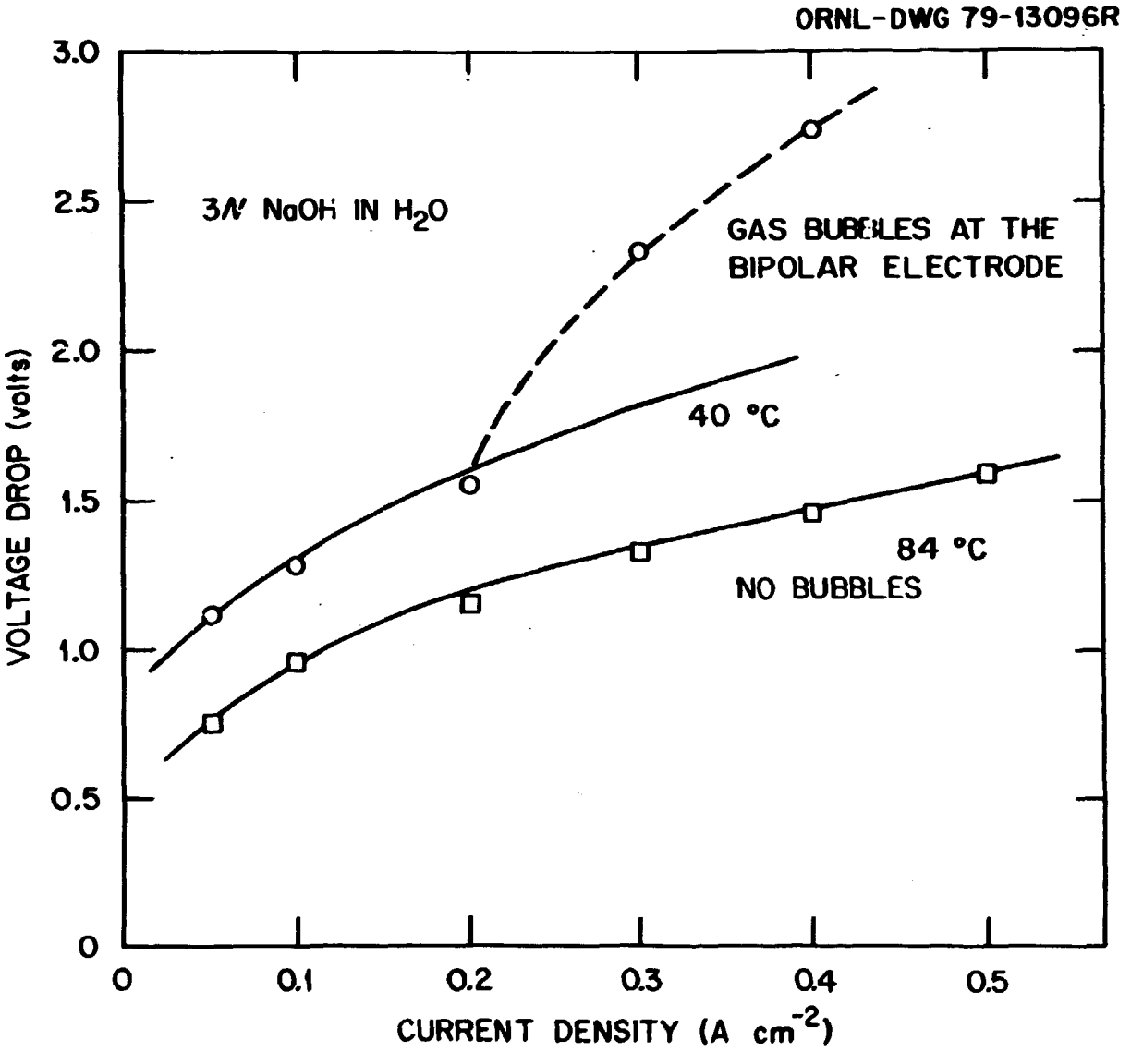

Figure 7. The effect of current density on the voltage drop through a 7.6×10^{-3} cm thick Pd-25% Ag bipolar electrode at 40 and 84°C. Gas bubbles appear at the electrode at current densities >0.2 A cm^{-2} at 40°C. Electrolyte: 6 N NaOH in H_2O.

maintained its trend with temperature change, with or without gas formation. A possible explanation of this phenomenon is that hydrogen gas is being formed simultaneously with Pd-H at the cathode surface, allowing the nature of the cathodic process to be essentially the same below and above the m.c.d. At the anodic surface, the supply of dissolved hydrogen in the electrode becomes insufficient, at currents exceeding m.c.d., to sustain the current flow. Therefore, another electrochemical process takes place simultaneously with hydrogen oxidation, namely, gaseous oxygen formation from water. This latter process results in an increased anode surface potential as compared to that observed where only hydrogen oxidation takes place. It should be noted that the anode surface voltage decreased similarly to that predicted theoretically: the m.c.d. curve for the 7.6×10^{-3} cm thick electrode has the value of 0.4 A cm^{-2} at 60°C (Fig. 5) exactly where the anode surface voltage decreases, as shown in Fig. 6. No gas formation was observed, as was predicted, for a 2.5×10^{-3} cm thick electrode through the entire temperature range at 0.4 A cm^{-2}.

The effect of current density on the voltage drop across the bipolar electrode is shown in Fig. 7. The advantage of operating the cell at a high temperature is immediately apparent: the voltage drop across the bipolar electrode decreases as the temperature increases and the m.c.d. can be maintained at a high value. By comparing Fig. 5 and Fig. 7, it can be seen that the experimentally observed gas formation between 0.2 and 0.3 A cm^{-2} at 40°C was theoretically predictable.

Similar behavior to that described above was found in the NaOD-D_2O system (see Figs. 7 and 8). Gas formation at the bipolar electrode at low temperature (40°C) was accompanied by an increased voltage across the

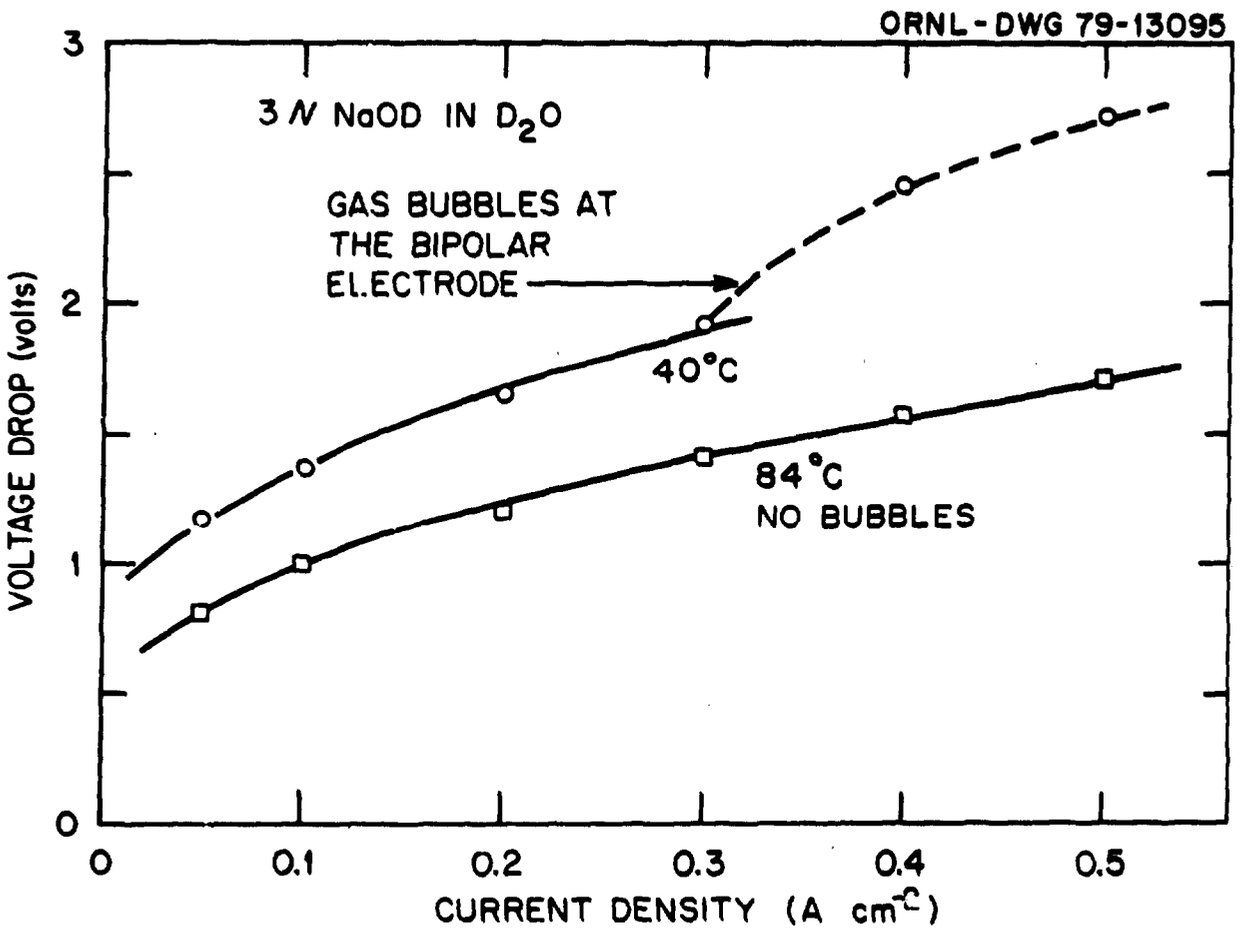

Figure 8. The effect of current density on the voltage drop through a 2.5×10^{-3} cm thick Pd-25% Ag bipolar electrode at 40 and 84°C in the D_2O-NaOD system. Gas bubbles appear at the electrode at 40°C and current densities >0.3 A cm^{-2}.

electrode. At high temperature (84°C) no gas formation was observed up to 0.5 A cm^{-2} current density. The effects of temperature and electrode thickness are shown in Fig. 9 for the H_2O-NaOH and the D_2O-NaOD system. Although the effect of electrode thickness is appreciable at low temperature, at temperatures above 60°C it becomes less pronounced.

A current density of 0.3 A cm^{-2} was applied successfully to a multi-bipolar cell furnished with four 7.6×10^{-3} cm thick bipolar electrodes at a temperature of 85°C for a period of 24 days without bubble formation. This experimental condition is found in Fig. 5 to lie below the m.c.d. curve, which further supports the theory. A series of experiments were performed at 0.210 A cm^{-2} and 0.350 A cm^{-2} in 99% D_2O and at 35, 50 and 90°C. At 0.210 A cm^{-2} very few bubbles were observed, but at 0.350 A cm^{-2} significant bubble formation was observed. From measured mass balance data, however, it appeared that less than 1% of the total current was consumed in gas formation. This is an additional indication that the D_2O system must be operated at a lower m.c.d. than the H_2O system.

Conclusions

Surface-treated Pd-25% Ag electrodes appear to be suitable for use in the bipolar hydrogen isotope separation process. A current density of 0.3 A cm^{-2} can be successfully applied for a prolonged period without bubble formation at the bipolar electrode surfaces; this current density is a four-fold increase over the reported m.c.d. on carbon electrodes (3) and a 70-fold improvement over the current densities achieved by Salmon (1) with Pd electrodes. Calculations indicate that current densities of 1 A cm^{-2} can be expected to be reached with thinner electrodes (2.5×10^{-3} cm)

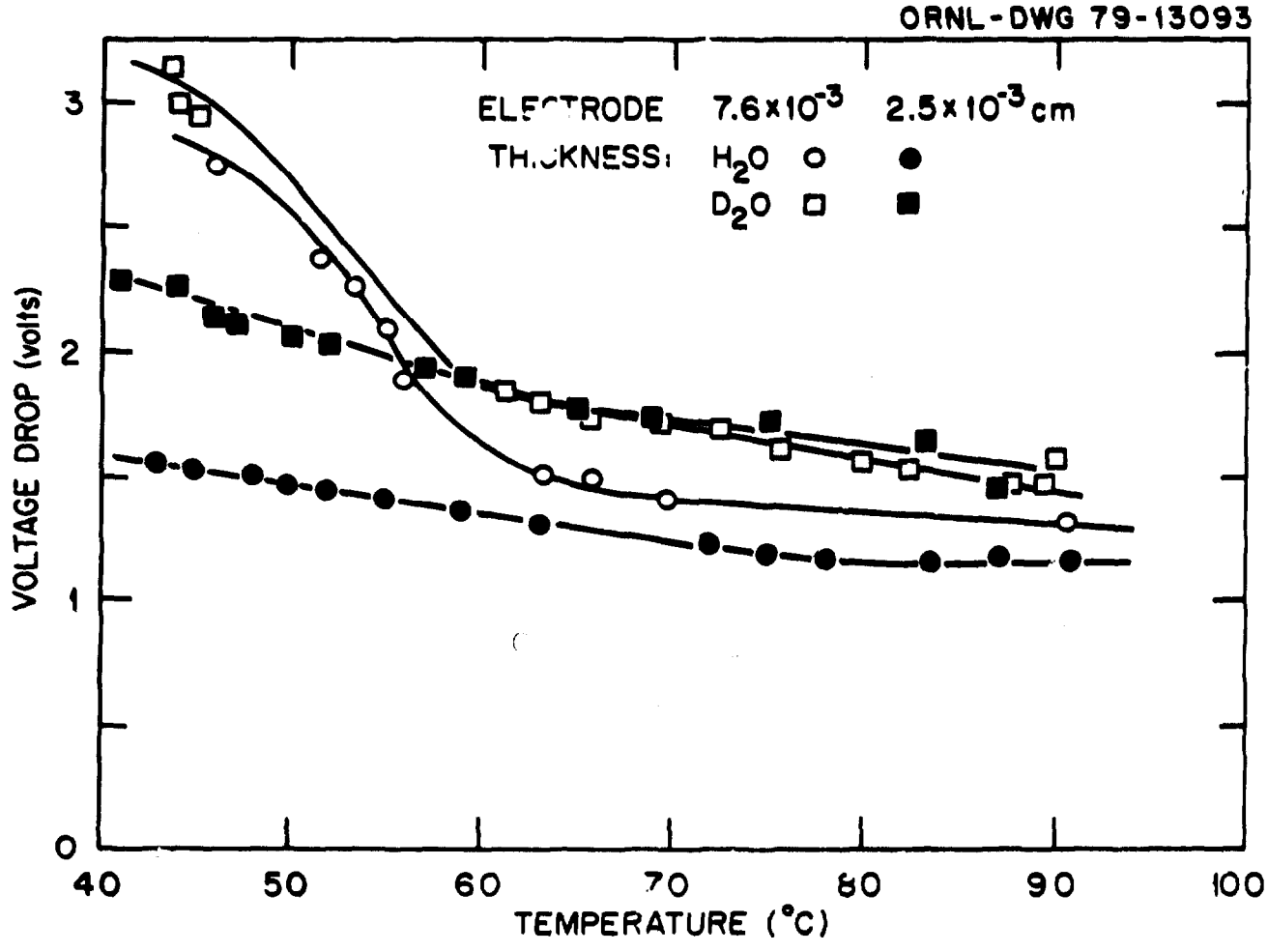

Figure 9. Comparison of the temperature dependence of the voltage drop across the bipolar electrode in the H_2O and the D_2O system. Current density 0.4 A cm^{-2}, electrode thicknesses: 2.5×10^{-3} and 7.6×10^{-3} cm. (Data are expressed as the sum of the anodic and the cathodic surface potential.)

at temperatures above 60°C. Long-term hydrogen permeation experiments (one year or longer) still must be performed in order to study potential permeation poisons and to determine the most appropriate surface activation methods.

Current densities in the range of 0.3 to 0.5 A cm^{-2}, which have been demonstrated as being achievable for the bipolar cell, would permit the required compact cell design and relatively small amounts of the electrode material to be used, thus making the process economically attractive.

The observed m.c.d.'s appear to be in reasonable agreement with calculated values. The increase in voltage drop across the bipolar electrode associated with the formation of bubbles may be used as an indicator of performance when visual observation is impractical.

POWER CONSUMPTION IN THE BIPOLAR PROCESS

Introduction

To achieve hydrogen isotope separation by conventional electrolysis, one must electrolyze water into its components: hydrogen and oxygen. In an equilibrium situation, i.e., where there is no net current flowing through the cell, the change in free energy ($\Delta G°$) of the overall chemical reaction may be expressed as

$$-\Delta G° = nFE°, \qquad (2)$$

where $E°$ represents the standard potential of the electrochemical reaction (20). For electrolysis of water at 25°C, $E° = 1.229$ V (21), which means that for an infinitestimally slow rate of water electrolysis the applied voltage must be greater than 1.229 V for the reaction to proceed:

$$H_2O \rightarrow 1/2\ O_2 + H_2. \qquad (3)$$

In terms of partial electrode reactions, Equation 3 can be separated into the cathodic process:

$$2\ H_2O + 2\ e^- \rightarrow H_2 + 2\ OH^- \qquad E^\circ = -0.828\ V \qquad (4)$$

and the anodic process:

$$2\ OH^- \rightarrow 1/2\ O_2 + 2\ e^- + H_2O \qquad E^\circ = -0.401\ V. \qquad (5)$$

At the bipolar electrode the separation of hydrogen isotopes is accomplished by the reduction and oxidation of hydrogen. At equilibrium, with no net current flowing through the system, the reaction at the cathode surface (22) is:

$$H_2O + e^- \rightarrow H(Pd) + OH^- \qquad E^\circ\ (red) \tilde{=} -0.8\ V. \qquad (6)$$

By definition (20), the reverse reaction, i.e., oxidation of hydrogen from the palladium surfaces, is as follows:

$$Pd\ (H) + OH^- \rightarrow H_2O + e^- \qquad E^\circ\ (ox) \tilde{=} +0.8\ V. \qquad (7)$$

On summing equations (6) and (7), no net reaction results, $\Delta G^\circ = 0$, and the standard potential $E^\circ = 0$. In other words the reaction can proceed at a voltage slightly greater than zero, as compared to conventional electrolysis where the voltage must be >1.23 V. This difference in E° permits considerable power savings when using hydrogen permeable bipolar electrodes as compared with normal electrolysis.

Voltage Distribution in the Electrolytic Cell

When current flows through an electrolytic cell, a voltage greater than E° must be applied to cause the reaction to proceed at some desirable rate. The magnitude of the cell voltage increases with current density and depends on the nature of the electrochemical processes at the anode, at the cathode, and on the resistance of the electrolyte between the

electrodes. Diagrammatic representation of typical cell voltage components is shown in Figure 10.

A highly conductive electrolyte must be used to minimize the IR drop; for the bipolar cell, 6N NaOH appears to be satisfactory. Potassium hydroxide has a slightly higher conductivity between 80 and 100°C than does NaOH, but the conductivity as a function of concentration for NaOH has some advantages over that of KOH (23,24). Although a strong acid would have a higher conductivity than NaOH, fewer corrosion problems occur with the alkaline medium. In Figure 11, the calculated IR drop for 6N NaOH electrolyte and at 1 cm electrode spacing is shown for current densities of 0.2 and 0.5 A cm^{-2} (which is within the expected range for an operating cell).

The electrode reaction contribution to the cell voltage can be expressed in terms of polarization or overvoltage. In general, polarization at an electrode under current flow is

$$\eta = E(i) - E(0) \qquad (8)$$

where E(0) is the voltage measured against a standard electrode with no current flowing and E(i) is the voltage at current density i. If only one electrode reaction takes place and the properties of the electrode do not change with current density then,

$$\eta = E(i) - E^{\circ} \qquad (9)$$

and η is called overvoltage (25). For the case of Pd-25% Ag electrodes, it is expected that the only electrochemical reactions which take place are hydrogen oxidation and reduction; however, E° of Pd-25% Ag is also a function of the hydrogen content of the alloy and can change by approximately 0.250 volts as hydrogen content varies from 0 to 0.26 H/metal (26).

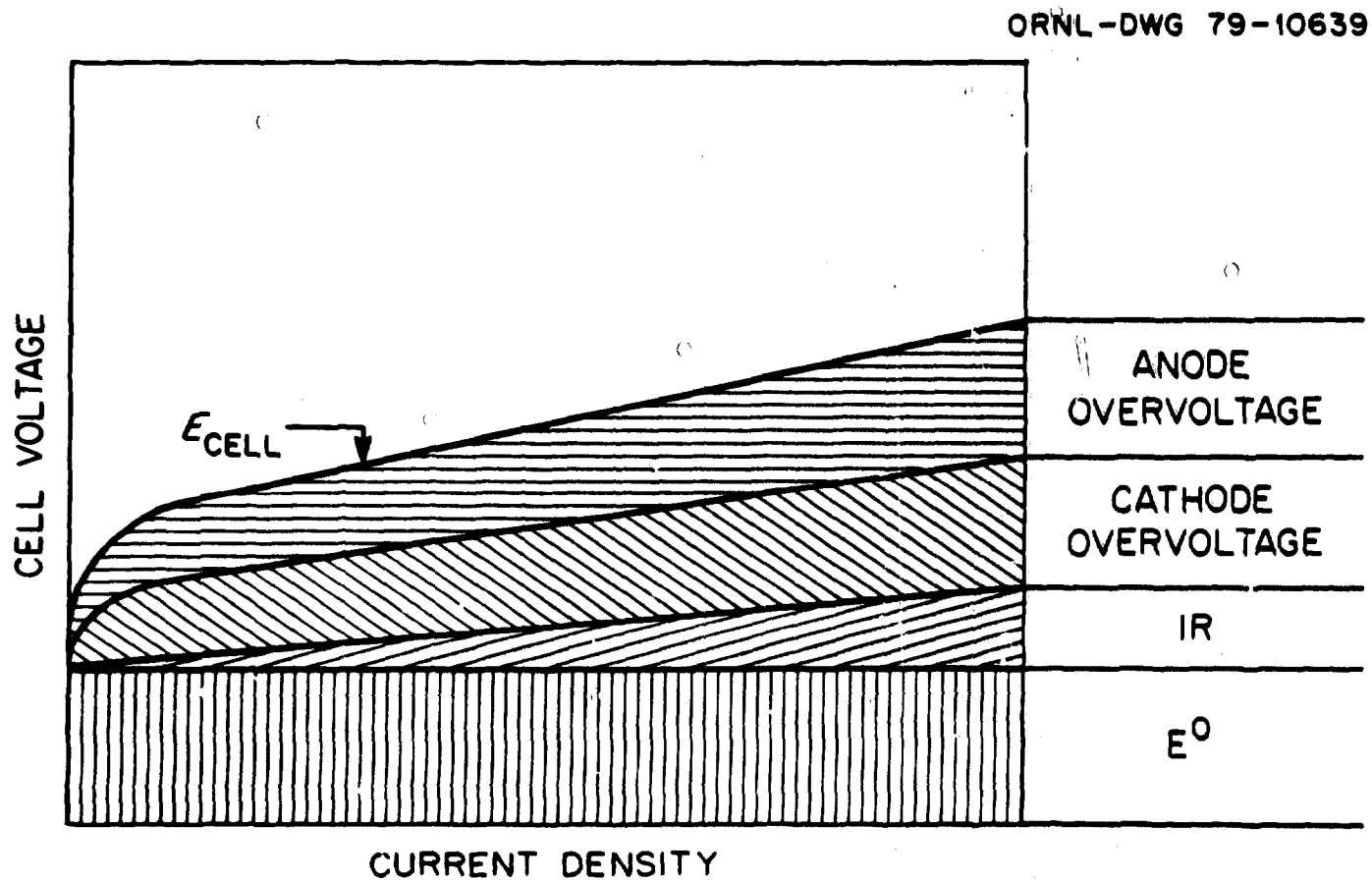

Figure 10. Voltage distribution within a typical electrolytic cell. Cell voltage is the sum of all partial voltage drops from one electrode to the other.

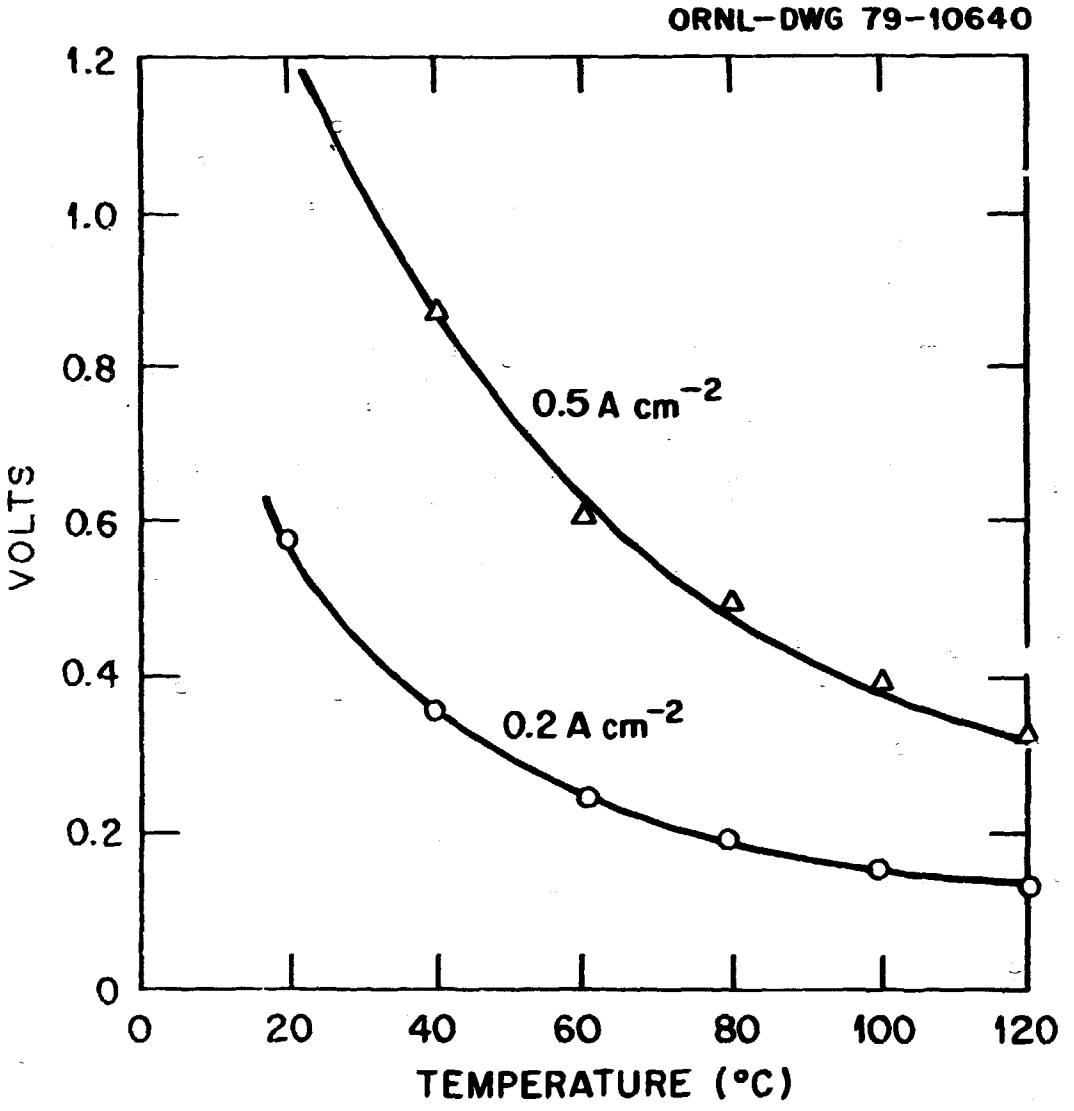

Figure 11. Voltage drop between two parallel electrodes at 1 cm distance caused by the electrolyte resistance. Electrolyte = 6 N NaOH, current density 0.5 and 0.2 A cm^{-2} (NaOH conductivity data from Ref. 23).

The cathodic surface overvoltage at the Pd-25% Ag membrane is expected to vary linearly with the logarithm of current density:

$$\eta = a + b \log |i| \quad (i < 0 \text{ for cathodic process}) \qquad (10)$$

The slope, b, depends on the overall stoichiometry of the rate-determining reaction and on the number of electrons involved. Polcaro et al. (26) proposed the following reaction sequence to describe the cathodic reaction of hydrogen on Pd-25% Ag:

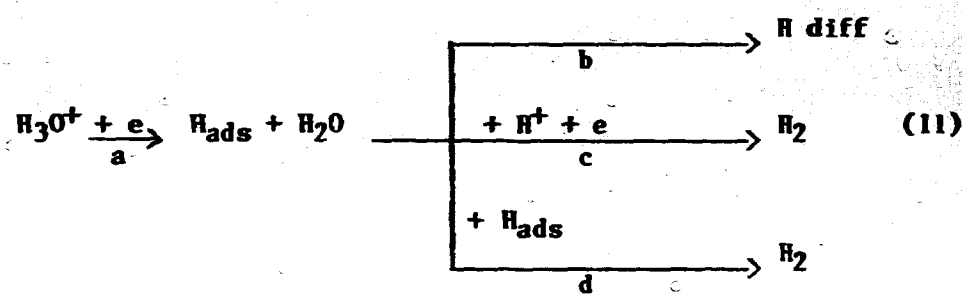

(11)

At low current densities, reaction "b", i.e., the diffusion of hydrogen from the cathode surface into the bulk metal was found to be the rate-controlling process. As a consequence, there was found to be a non-linear dependence of overvoltage on the logarithm of current density, since a simultaneous change in E° took place because of initial increasing hydrogen content of the alloy with time. As the cathode surface became saturated with hydrogen, E° reached a constant value, reaction "c" became rate determining, and a linear slope of approximately 0.12 V was found. Studies of anodic overvoltage of a hydrogen-saturated Pd-25% Ag electrode showed an exponential dependence on the logarithm of current density indicating that the diffusion of hydrogen out of the metal (reversed reaction b and a) was the rate-determining step at the anode surface.

The current density-voltage relationship for a Pd-25% Ag electrode has not been studied in the bipolar system. Some studies done on pure palladium electrodes in acid solutions, relating to the permeability of hydrogen through the electrode (9,10,27), can be related to the Pd-25% Ag system. Von Stackelberg and Ludwig (10), in experiments described in the previous chapter, found that the voltage drop across the bipolar electrode was >1.4 V at a current density of 0.27 A cm^{-2} (exact numbers were not given).

Hoare and Schuldiner (27) studied the effect of electrode thickness on the palladium bipolar electrode behavior in sulfuric acid solutions and found that at 0.01 A cm^{-2} the voltage drop across the electrode changed by 0.075 V when the electrode thickness was changed from 2.5×10^{-3} to 9.2×10^{-3} cm. However, at higher current densities, this difference was much larger and most of the increase occurred at the anodic surface. Such behavior can be explained by a hydrogen concentration gradient through the palladium electrode: it varies linearly with distance into the electrode as shown in Figure 12 (if only one phase of hydrogen palladium is present)*. At the anode surface of a thin electrode there would be an appreciable amount of dissolved hydrogen available. Since the potential at the electrode is not a linear function of the concentration of the electroactive species at the surface, a small change in hydrogen content at the anode surface can cause a large change in overvoltage.

---

*This is particularly valid for the palladium-silver-hydrogen system where only one phase exists in the entire hydrogen concentration range.

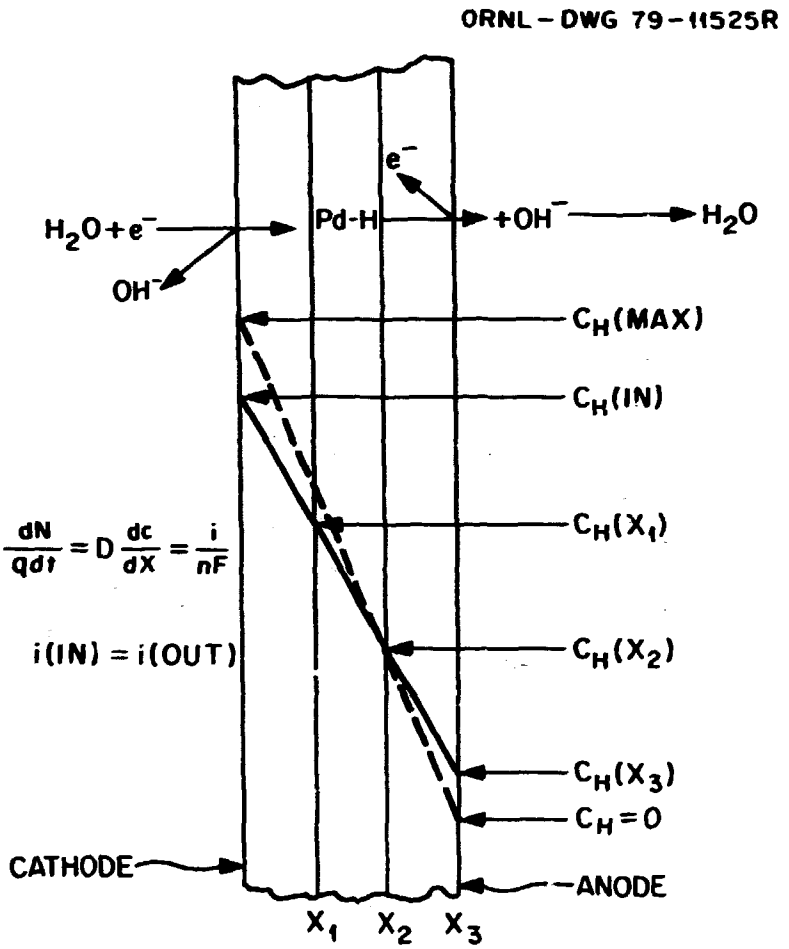

Figure 12. Hydrogen concentration profile in a Pd-25% Ag bipolar membrane at constant current conditions. Maximum current density is defined by

$$i = nFD \frac{C_H\ (max)}{X},$$

X_1, X_2, X_3, = electrode thickness (cm)
C_H = hydrogen concentration in the alloy (mole cm^{-3})
N = number of moles
q = cross section area (cm^2)
D = diffusion coefficient ($cm^2\ sec^{-1}$)
F = faraday (95,600 coulombs/equivalent)
n = number of electrons transferred/mole
i = current density (A cm^{-2})
t = time (sec)

Experimental Results and Discussion

Experiments with a small thermostated bipolar cell (Fig. 2), as described in the previous chapter, will now be discussed from a power consumption point of view. The temperature dependence of the anode surface voltage and the cathode surface voltage was measured at a constant current density of 0.4 A cm^{-2} (Fig. 6). Two electrode thicknesses were tested. At an electrode thickness of 2.5×10^{-3} cm, both anode and cathode surface voltages showed a slight decrease with increasing temperature; with 7.6×10^{-3} cm thick electrodes, the anode surface voltage was high at low temperatures (2.3 V vs. Pd-H electrode in the same electrolyte at 40°C) and diminished quickly with increasing temperature. Practically the same voltage values were reached with the thicker electrode as with the thinner one at temperatures above 60°C. The cathode surface voltage for the thicker bipolar electrode was about 0.1 V more negative than the other. The high voltage at the anode surface at low temperature was accompanied by bubble formation on both sides of the bipolar electrode. This indicated that the m.c.d. value had been exceeded; more hydrogen was formed at the cathode surface than was able to penetrate through the electrode and the surplus was evolved in the form of gas. An equivalent amount of oxygen was evolved at the anode surface. For reasons described earlier (p.20), when oxygen was generated at the anode surface, the anode potential assumed a value between the hydrogen and the oxygen evolution potential. It is therefore important to operate the cell at enhanced temperature and with thin electrodes so as to have total hydrogen permeability and minimum power consumption.

These experiments are of a preliminary character. However, data presented in Figs. 6, 7, 8, and 9 are reproducible within the error limit ($\pm$3°C, $\pm$10 mV) and can be used to judge electrode performance.

In Figs. 7-9 the total voltage drop across the bipolar electrode (the sum of the anode and cathode surface voltages) was plotted as functions of current density and temperature, respectively. From these data it was concluded that the minimum power needed to operate the process would be achieved at temperatures above 70°C with thin electrodes. Electrolysis in the D_2O system would require somewhat higher voltage and consequently more power than for the H_2O system.

During continuous cell operation using multibipolar electrodes, the total voltage drop through one bipolar membrane (after several hours at 0.3 A cm^{-2} and at 60°C) was measured to be 1.77 $\pm$0.06 V, while after three weeks of operation it was found to have increased to 1.88 $\pm$0.06 V. In this case the bipolar electrodes were 7.6×10^{-3} cm thick and the electrolyte was 2 N NaOH. The relatively high voltage drop at the bipolar electrode during continuous operation can be attributed to the low operating temperature (60°C), electrode thickness, and gradual accumulation of traces of impurities at the electrode surface. In early experiments it was observed that current reversal in the cell for a few seconds re-established a reduced bipolar voltage.

Power consumption associated with the bipolar process can be assessed provided two basic parameters are established: the total amount of water needed to be electrolyzed in order to achieve a given enrichment (or depletion) and the electric power consumed in the process per unit amount of water electrolyzed. The first parameter depends on the specific

application, i.e., whether tritium is to be removed from light or from heavy water (difference in separation factor) and also on the tritium concentration in the feed stream, as well as the desired tritium concentration in the enriched and depleted streams leaving the cascade. This parameter will be discussed later.

Electric power consumption is dependent on the current density; the greater the current density the higher the voltage drop in the electrolyte and the higher the overvoltage at the electrode surface. To minimize power consumption, it would be best to operate the cell at low current density, but from the standpoint of capital investment and containment cost, high current densities must be achieved. For each particular application, the most appropriate operating current density must be determined.

Most normal electrolytic processes do not operate at current densities exceeding 0.2 A cm^{-2} at which the corresponding power consumption is approximately 6.4 kwh/kg H_2O (28-31). Using measured overvoltage at the currently developed bipolar electrodes, power consumption for one stage of bipolar electrolysis at 0.2 A cm^{-2} was estimated to about 3 kwh/kg H_2O (0.9 V at a 2.5 x 10^{-3} cm thick bipolar electrode, and 0.12 V resistive loss between the electrodes using 6 N NaOH, 90°C and a 0.6-cm electrode spacing). At a current density of 0.5 A cm^{-2}, the power consumption of one bipolar electrolysis stage would increase to about 5 kwh/kg H_2O (1.2 V at the electrode, as shown in Fig. 9, and 0.3 V resistive loss between electrodes). Large scale electrolyses usually do not operate at such high current density. If the reported voltage requirements for normal electrolyses are extrapolated to a current density of 0.5 A/cm^2, then power consumption would increase to about 8 kwh/kg

H_2O. This estimate of BPE power consumption does not include cell voltage increases with time which usually occur caused by changes in electrode surface activation during continuous operation. The amount of such time-dependent increase must be studied experimentally and its cause determined so as to prevent or reduce its effect on power consumption.

Conclusions

Measurements of voltage drop across the bipolar electrode indicate that the power consumption associated with a single bipolar stage at a current density of 0.2 A cm^{-2} is only about 45% of that required for normal electrolysis of the same amount of water; for a current density of 0.5 A cm^{-2}, the power consumed would be about 60% of that required for normal electrolysis. These power estimates require confirmation in long-term experiments. Total power consumption of the BPE process can be estimated by combining the estimated power consumption per kilogram of water with the total amount of water required to be electrolyzed as determined by the application.

SEPARATION FACTORS

Introduction

The hydrogen isotope separation factor is defined as

$$\alpha = \frac{Y}{X} \quad ; \text{ or } \alpha = \frac{y/(1-y)}{x/(1-x)} \tag{12}$$

where Y = mole ratio of the light isotope to heavy isotope in the heavier isotope-depleted phase (gas phase for conventional electrolysis; hydrogen penetrating the bipolar membrane for bipolar electrolysis)

X = mole ratio of the light over the heavy isotope in the remaining phase (aqueous phase remaining in the electrolytic cell for conventional electrolysis; aqueous phase remaining in the interelectrode compartment for bipolar electrolysis)

y,x = mole fractions of the light isotope in the depleted and remaining phase, respectively.

The electrolytic protium-deuterium separation factor, α_{HD}, is of interest mainly because of the possible application of BPE to heavy water production. Historically, the necessity of determining the protium-tritium separation factor, α_{HT}, arose when the concentration levels of naturally occurring tritium was of interest to a variety of researchers. Tritium concentration levels in nature are too low to be determined by direct radiation counting, and thus concentration by batch-type electrolyses was required for such determinations. The original tritium content only could be determined by this technique when α_{HT} was known (33).

A mathematical relationship between the protium-deuterium and protium-tritium separation factors was derived by Bigeleisen (34):

$$\frac{\ln\alpha_{HT}}{\ln\alpha_{HD}} = 1.38 + \frac{0.06}{\ln\alpha_{HD}} \quad . \tag{13}$$

This relationship has been confirmed for a wide range of experimental conditions (33,35). Thus, the deuterium-tritium separation factor can be calculated if α_{HT} and α_{HD} are known:

$$\alpha_{DT} = \frac{\alpha_{HT}}{\alpha_{HD}} . \tag{14}$$

Consequently, by knowing one of the separation factors under specific experimental conditions, the other two may be estimated adequately from Eqns. 13 and 14. The values of hydrogen isotope separation factors are found to vary over a broad range depending upon the electrode material, current density (or overvoltage), and temperature. Some reported values for α_{HD}, α_{HT} and α_{DT} using normal electrolysis are given in Table Ia. In most cases, the heavy isotope concentration in the electrolyte was very low as compared to the protium content, but in some experiments comparable concentrations of protium and deuterium were used (14, 36, 37). The difference in hydration energy for an isotope hydrated predominantly with H_2O, DHO, or D_2O can be an additional source of variance in α_{HD} values (38,39). The effect of the electrode reaction mechanism on separation factor as a function of hydrogen evolution at metal electrodes was studied by Conway (38), and Bockris (39).

In conventional electrolysis the hydrogen evolution mechanism can be described by the following reactions:

$$H_3O^+ + e^- + M \rightarrow MH_{ads} + H_2O \quad (15)$$

$$H_3O^+ + e^- + MH_{ads} \rightarrow H_2 + H_2O + M \quad (16)$$

$$H_{ads} + H_{ads} \rightarrow H_2 \quad (17)$$

$$H_2O + e^- + M \rightarrow HM_{ads} + OH^- \quad (18)$$

Table 1a. Electrolytic Hydrogen Isotope Separation Factors

Electrode Material	Current Density (A cm^{-2})	Electrolyte	Temperature °C	α_{HD}	α_{HT}	α_{DT}	Reference
Fe Foil	-	KOH	20	7.3	12.0	1.64*	(37)
Fe Sinter	0.1	KOH	20	6.1	11.1	1.82*	(37)
Fe-Ni Sinter	0.1	KOH	20	7.7	16.2	2.10*	(37)
Pt	0.1	KOH	20	7.7	17.1	2.22*	(37)
Hg	0.1	H_2SO_4	20	3.3	5.1	1.54*	(37)
Mild Steel	-	KOH	25-35	8-9	-	-	(42)
Carbon	Var.	NaOH	25-60	-	16-22	-	(3)
Pt	Var.	NaOH	25-60	-	17-21.5	-	(3)
Pd-25% Ag Tubes	0.02	K_2CO_3 in 80-90% D_2O	0	13.1	-	-	(14)
Pd-25% Ag Tubes	0.02	K_2CO_3 in 80-90% D_2O	20	10.3	-	-	(14)
Pd-25% Ag Tubes	0.02	K_2CO_3 in 80-90% D_2O	40	9.1	-	-	(14)
Pd-25% Ag Tubes	0.02	K_2CO_3 in 80-90% D_2O	60	7.8	-	-	(14)
Mild Steel	0.01	KOH	0.5	11.7	31.8	2.7*	(35)
Mild Steel	0.01	KOH	22.5	9.6	24.9	2.6*	(35)
Mild Steel	0.01	KOH	40	8.0	19.5	2.4*	(35)
Mild Steel	0.01	KOH	60	6.7	15.0	2.2*	(35)
Stainless Steel or Ni Screen	Var.	KOH in H_2O-D_2O Mixture		4.0	6.9	1.7	(36)

*Calculated from $\alpha_{DT} = \frac{\alpha_{HT}}{\alpha_{HD}}$.

With different electrodes and different current densities the mechanisms may vary, causing variations in the separation factor. Lewis and co-workers (40) determined the electrolytic separation factors for various metal electrodes and found that the separation factors were a non-monotonic function of applied overvoltage.

From the temperature dependence of the separation factors, the differences in the activation energy for the discharge of a particular isotope pair can be calculated (35):

$$\frac{d \ln\alpha}{d T} = \frac{\Delta H_{\alpha}}{RT^2} , \qquad (19)$$

where T is the temperature in °K, R is the gas constant and α is the separation factor for the particular pair of hydrogen isotopes. By plotting ln α vs. 1/T, straight lines were obtained and from their slopes the related ΔH could be determined. Roy (35) found the following values: $\Delta H(\alpha_{HD}) = -1680$, $\Delta H(\alpha_{HT}) = -2260$, and $\Delta H(\alpha_{DT}) = -580$ cal mol^{-1} at a current density of about 0.01 A cm^{-2}. From the data of Brodowsky et al. (14), a value of $\Delta H(\alpha_{HD}) = -1534$ cal mol^{-1} was calculated (applied current density of 0.02-0.023 A cm^{-2}).

The only studies of isotope separation factors arising in <u>bipolar</u> electrolysis were performed by Salmon (1) and Drazic (3) (see Table Ib). Drazic (3) determined the protium-tritium gas evolution separation factor for simple electrolysis on composite carbon electrodes and found a maximum value of about 22.5 (at 25°C and low overpotential). The separation factor for a single bipolar electrode for protium-tritium was much lower (about 8), which was attributed to dilution occurring by isotope exchange

Table 1b. Hydrogen Isotope Separation Factors on Bipolar Electrodes

Electrode Material	Current Density ($A\ cm^{-2}$)	Electrolyte	Temperature °C	α_{HD}	α_{HT}	α_{DT}	Reference
Pd	0.006	H_2SO_4	25	4.5	-	-	(1)
Carbon	0.06	NaOH	Room?	-	8	-	(3)
Pd-25% Ag	0.21-0.5	NaOH in H_2O or NaOD in D_2O	35	-	-	2.16	This work ORNL
Pd-25% Ag	0.21-0.5	NaOH in H_2O or NaOD in D_2O	55	5.9*	12.4	2.11	This work ORNL
Pd-25% Ag	0.21-0.5	NaOH in H_2O or NaOD in D_2O	90	5.7*	11.6	2.05	This work ORNL

*Calculated using $\alpha_{DT} = \frac{\alpha_{HT}}{\alpha_{HD}}$

in the vapor phase within the porous electrode. (The values for the separation factors are merely stated by Drazic with no explanation of how these values were measured. Little experimental data were given and the current density was <0.07 A cm^{-2}.) Salmon (1) obtained values of the protium-deuterium separation factor between 4 and 5 using a palladium bipolar electrode at room temperature in a sulfuric acid solution at 0.006 A cm^{-2}. Wicke and co-workers (14) examined partial separations taking place during the transport of hydrogen through a Pd-25% Ag membrane:

1. Electrochemical reduction at the cathode surface,
2. Diffusion of hydrogen through the bipolar membrane, and
3. Reoxidation of hydrogen.

The first two steps noted above are identical to reactions (15) or (18), and "b" in Equation (11). Wicke and co-workers performed the following sequence of experiments:

1. A Pd-25% Ag foil was used as a cathode in contact with electrolyte on only one side; the electrolyzed protium-deuterium isotope mixture was diffused through the electrode into the gas phase. Separation factors were determined from the isotopic composition of the aqueous phase and from the composition of the permeating gas. Values of the cathodic separation factor were found to be 13.1 and 7.8 at 0 and 70°C, respectively.
2. The above experiment (1) was reversed such that the hydrogen isotope mixture was diffused from the gas phase

through a Pd-25% Ag membrane, acting as an anode, and was subsequently oxidized at the anode-electrolyte interface. The anodic separation factor was found to be independent of temperature and varied between 1.64 and 1.84.

3. Values for α_{HD} of about 1.7 were obtained when a 1:1 H/D mixture was diffused through a Pd-25% Ag membrane (gas phases only on each side of the membrane).

Consequently, it would appear that the largest separation factor is associated with the electrochemical reduction mechanism and this may be somewhat enhanced by diffusion and reoxidation mechanisms.

Experimental Results and Discussion

Early in our studies of the bipolar process, separation factors arising at the bipolar membrane were measured. The experimental procedure used is illustrated in Fig. 2; the electrolyte solution containing a tritium tracer was placed in both the anode and cathode compartments. Initial conditions were determined, i.e., the total amount of water, concentration of KOH in both compartments and the initial tritium activity in both compartments. During electrolysis, a mixture of hydrogen isotopes passed from the anode compartment into the cathode compartment through the bipolar membrane. The exit "stream" of hydrogen leaving the anode compartment was found enriched in the light isotope and thus tritium was being concentrated in the anode compartment. Figure 13 illustrates the change in anode and cathode compartment compositions for a typical protium-tritium separation experiment. From changes in water volume and

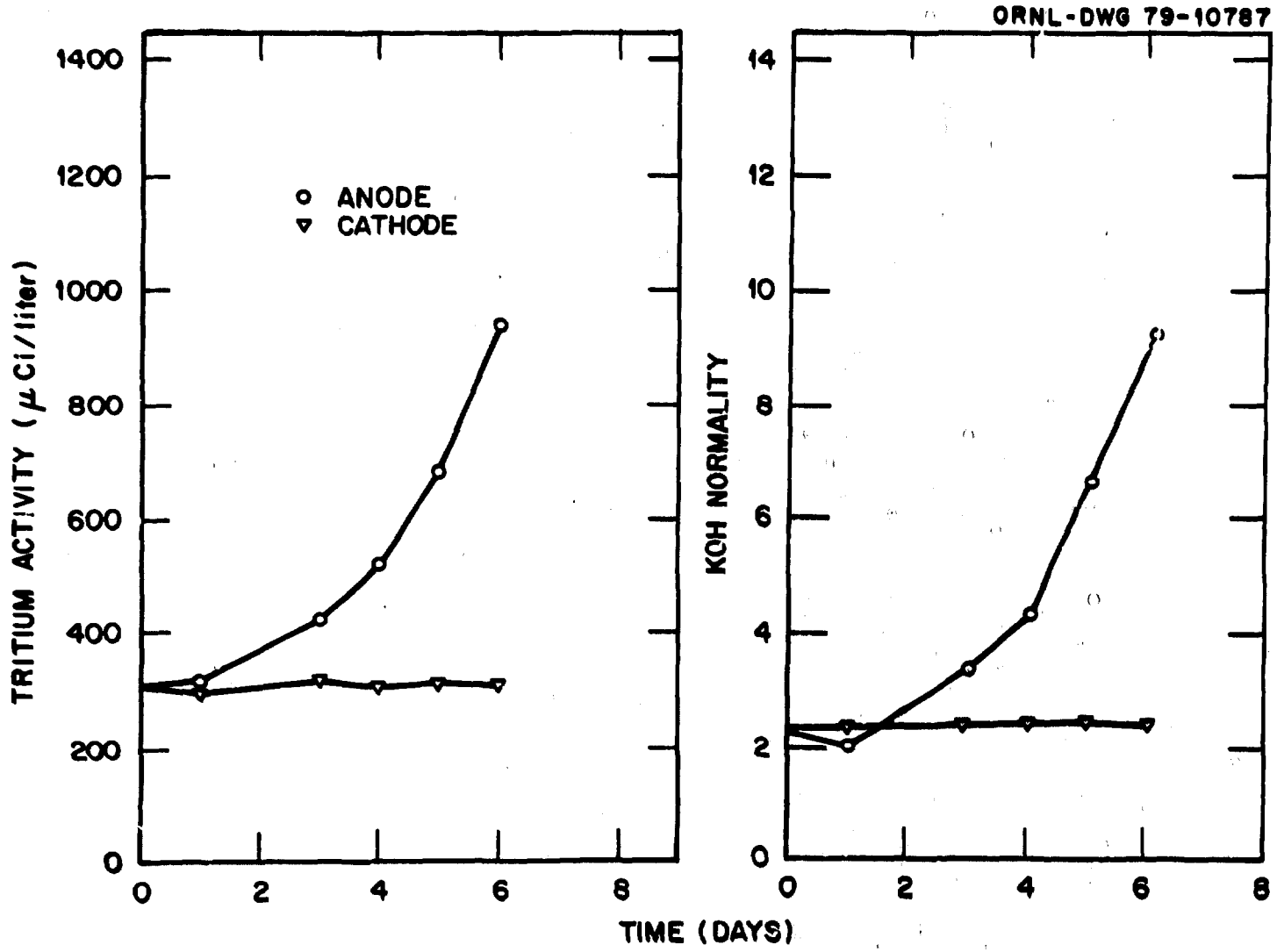

Figure 13. Changes in anode and cathode compartment composition for a typical protium-tritium bipolar electrode separation experiment.

tritium activity level in the anode compartment, the separation factor was calculated using the Rayleigh (41) formula:

$$\alpha_a = 1/\left[1 - \frac{\ln(A_a/A_{ao})}{\ln(W_{ao}/W_a)}\right], \qquad (20)$$

where A_{ao} and A_a are the initial and final tritium activity levels and W_{ao} and W_a are the initial and final moles of the lighter isotope in the anodic compartment. Small errors in determining either A or W resulted in very large errors in α. The determination of α from changes in the isotopic composition of the cathode compartment is complicated by two processes operating simultaneously: the influx of an isotopic mixture through the bipolar membrane and the removal of a different isotopic mixture at the terminal cathode. The net change in isotope composition in the electrolyte is affected by both separation processes. To circumvent this problem, hydrogen gas produced at the terminal cathode was continuously converted into water and returned to the cathode compartment, thus nullifying the isotope separation contributed by the terminal cathode. Under these conditions, α could be determined from the change in the isotopic composition of both anodic and cathodic compartments according to the relationship

$$\alpha_c = \frac{\ln W_a - \ln W_{ao}}{\ln[A_{ao} W_{ao} - A_c W_c + A_{co} W_{co}] - \ln A_{ao} W_{ao}} \qquad (21)$$

*Derivation of Equations (20) and (21) is given in Appendix B.

Using Equation (21) rather than Equation (20), the separation factors could be determined with much greater precision. This is illustrated in Figure 14 for a hypothetical experiment in which fixed values for all variables except W_a were assumed. It is evident that a small error in W_a causes large variation in α when Equation (20) is used.

Most of our experiments emphasized the measurement of α_{DT}, the separation factor on a single bipolar electrode for the deuterium-tritium isotope pair. The results obtained at three different temperatures at current densities of 0.21, 0.36, and 0.50 A cm^{-2} are given in Table 2. These data represent the average values of twenty-five individual experiments. The value of ΔH_{DT} calculated from the temperature dependence of α_{DT} was -190 cal mol^{-1}, which is considerably lower than the reported value of -580 cal^{-1} (14). It is not clear whether this difference is caused by much higher current densities applied in our experiments (0.21-0.50 A cm^{-2} compared to 0.01 A cm^{-2} in [14]), or to the bipolar process. More experiments are needed to clarify this difference. No significant dependence of α_{DT} on current density was found. Several measurements of α_{HT} were also made and the results are presented in Table 2; these values agree reasonably well with those predicted by Equation 13.

Table 2. Hydrogen Isotope Separation Factors on a Single Bipolar Electrode

Temperature °C	α_{DT} (0.21, 0.35, 0.50 A cm^{-2})	α_{HT} (0.35 A cm^{-2})	α_{HT} Calculated From α_{DT}
35	2.16 ± 0.06	-	-
55	2.11 ± 0.05	12.4 ± 1.3	12.9
90	2.05 ± 0.06	11.6 ± 0.7	10.7

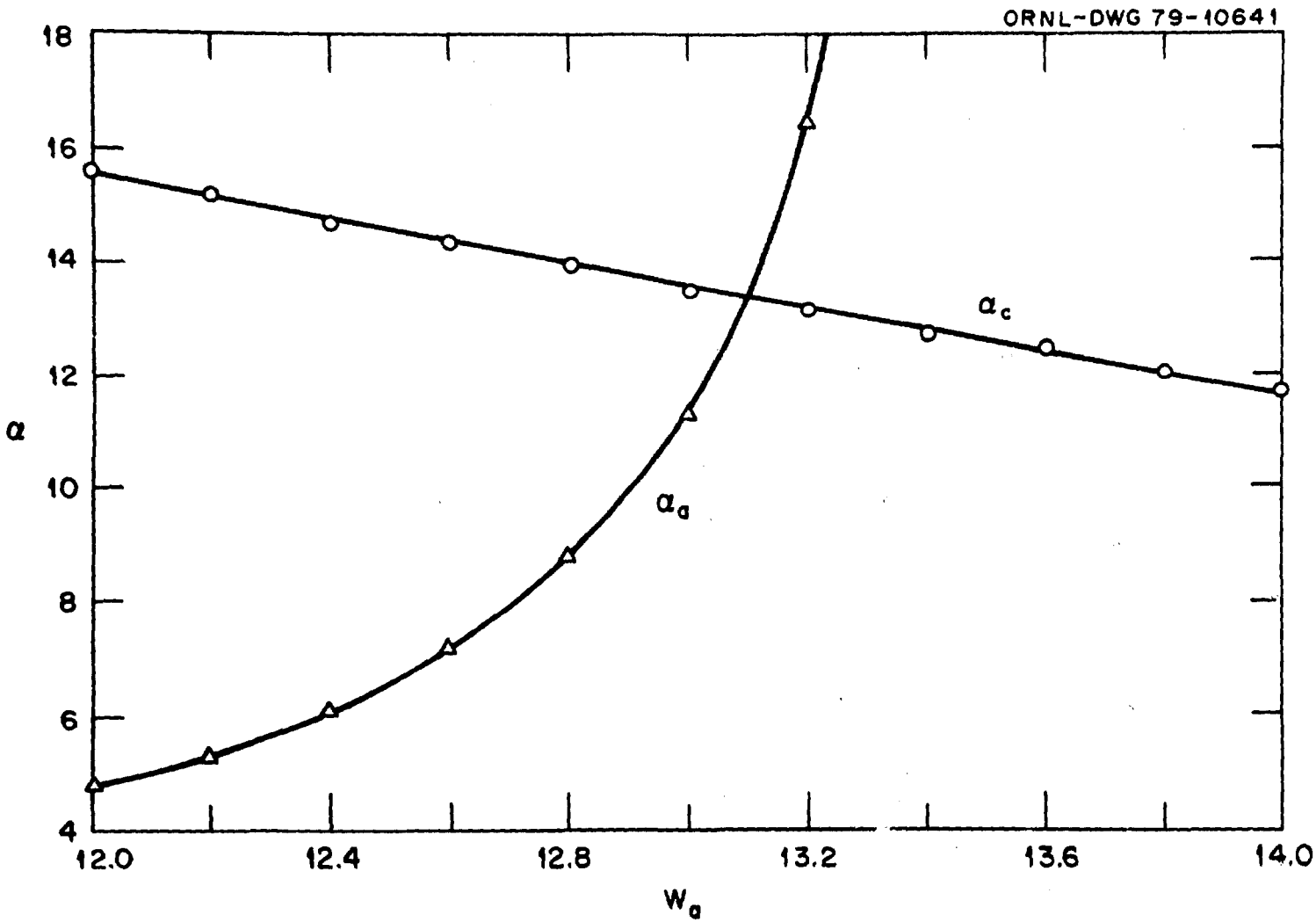

Figure 14. Values for α_{HT} at constant W_{ao}, A_{ao}, A_a, W_{co}, W_c, A_{co}, A_c (Equations 20 and 21) at various values of W_a.

In order to compare separation factors as measured using normal electrolysis and bipolar electrolysis, one half of the cell, as shown in Fig. 2., was filled with electrolyte (sodium hydroxide) containing a trace quantity of tritium. Palladium-25% silver foil served as the cathode. The back of the cathode foil was painted to prevent hydrogen from diffusing through the foil. Current density of 0.35 A cm^{-2} was applied to this "half-cell". Hydrogen gas evolving from the cathode was converted to water, and the H-T separation factor calculated from the isotopic composition of the reconstituted water as compared with the composition of the water remaining in the cell. Separation factor values of 8.6 $\pm$ 0.2 and 8.1 $\pm$ 0.2 for 55° and 90°C, respectively, were measured. These results show that under identical experimental conditions, the H-T separation factors for the bipolar process (see Table 2) were about 25-30% greater than that observed for the simple electrolytic process.

Since it has been shown that the mathematical relationship between the three separation factors (α_{HD}, α_{DT}, α_{HT}) is valid for both bipolar and normal electrolysis, it is anticipated that α_{DT} and α_{HD} will also be about 25-30% greater for the bipolar process.

Conclusions

The bipolar hydrogen isotope separation factors (α_{HT}, α_{DT}) were found to be within the expected range (see Table I) under experimental conditions as required in the proposed bipolar process: Pd-25% Ag electrode composition, high current density (0.2-0.5 A cm^{-2}), electrolyte concentration of 6 N NaOH, and a cell temperature of 60-90°C. The fact that the deuterium-tritium separation factor does not change appreciably with

neither temperature (between 35 and 90°C) nor current density, (between 0.21 and 0.50 A cm^{-2}) is a very important positive feature: incidental fluctuations in either current density or temperature would not result in significant changes in the separative process. Mathematical relationships between the three separation factors, valid for simple electrolysis (Equations 13 and 14), were found to be valid for bipolar electrolysis as well. For preliminary calculations of the cascade design, an $\alpha_{DT} = 2$ and $\alpha_{HT} = 11$ can be used.

Further studies are required to understand completely the difference in temperature dependence of separation factors as measured in bipolar and simple electrolytic systems.

INTERSTAGE SEPARATION

Introduction

Steady-state cascade theory is concerned with the prediction of the stage requirements for the separation of a given isotope mixture into products of specified composition. Such calculations give the number of stages needed for desired separation, the local interstage flowrates and compositions, total separation for a given cascade, and other design details.

The bipolar electrolysis cascade is inherently "square"; the electrode area of each stage is the same throughout the cascade. Due to subtle differences between bipolar cascade design and conventional cascade modeling, it is necessary to derive design equations specifically for bipolar electrolysis. Appendix C gives a detailed derivation of these

equations for the enriching section of a BPE square cascade for one type of flow scheme.

Total enrichment (i.e., total increase in heavy isotope concentration from feed to product) for the enriching section of a square BPE cascade with the flow scheme as noted in Appendix 3 may be expressed as

$$m_F = \beta m_p,$$

$$\beta = (1/\alpha\phi)^J + \frac{P}{F}\left[\frac{1 - (1/\alpha\phi)^J}{1 - (1/\alpha\phi)}\right], \qquad (22)$$

where

m_F = mole fraction of heavy isotope in the feed,

m_p = mole fraction of heavy isotope in the product,

$\alpha = \frac{1}{1 - P/F}$,

= single stage bipolar separation factor,

P = molar flowrate of product, has the units of total moles of hydrogen*/unit time,

F = molar flowrate of feed; has the units of total moles of hydrogen/unit time,

J = total number of separation stages in a square section with stage number one being the bipolar electrode opposite the terminal anode.

Equation (22) may be used to calculate the number of stages (J) necessary to enrich a heavy isotope to a desired concentration. Also, equation (22)

---

*Total moles of hydrogen--the total molar flowrate of any two hydrogen pairs: $H_2 + T_2$, $H_2 + D_2$ or $D_2 + T_2$.

may be used to calculate the interstage isotope composition in the electrolyte throughout a square cascade with a given product composition (m_p), single stage separation factor (α), and product-to-feed ratio (P/F). To use Equation (22) in calculating interstage composition, the term m_F may be considered as the feed composition of stage J, which is in reality the interstage composition between the J and J + 1 stages (see Fig. 15).

It is of particular interest to examine interstage composition (m_p) with respect to variations in α and P/F. Figure 16 is a family of curves which illustrates the interstage compositional variation with respect to change in separation factor for a constant P/F. It should be noted that each curve exhibits a point of inefficient operation at which no appreciable enrichment occurs with the addition of more separative stages. For large separation factors ($\alpha \geq 10$), it can be seen that this point of inefficient operation is reached in a very few stages.

Figures 17 and 18 show a family of curves which illustrate the interstage compositional variations with respect to changes in P/F at a constant separation factor. Ratios (P/F) of 1×10^{-1} to 2×10^{-2} imply a product withdrawal rate 10 to 50 times less than the feed rate. This P/F range is appropriate for both laboratory and large-scale applications. For a given separation factor, the smaller the value of P/F the greater is the number of stages that can be efficiently utilized in a square cascade, and for a large separation factor (i.e., protium-tritium or protium-deuterium) relatively few stages can be efficiently utilized in any single square section of a cascaded system.

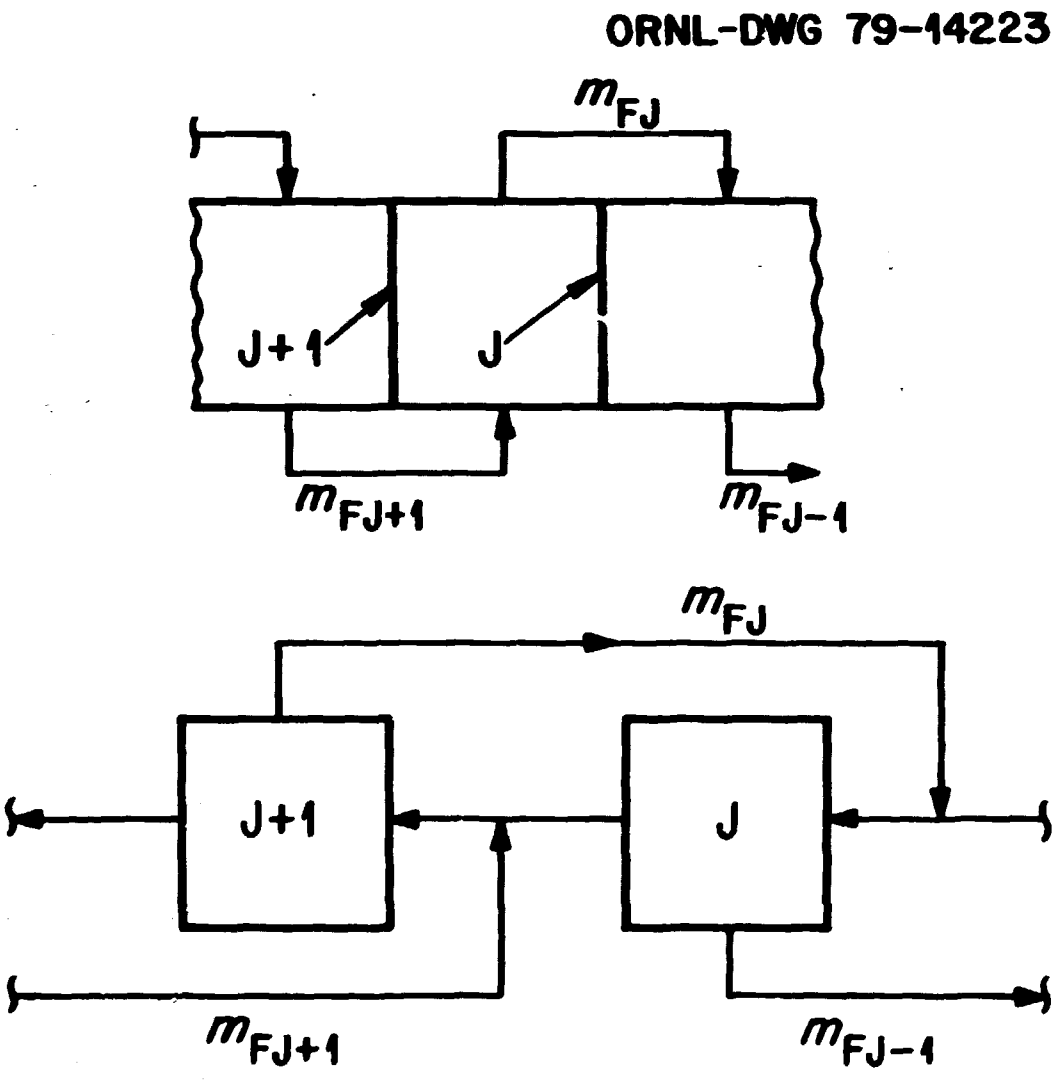

Figure 15. Stage to stage nomenclature illustrating that the enriched product of the J + 1 stage is the feed for the J'th stage.

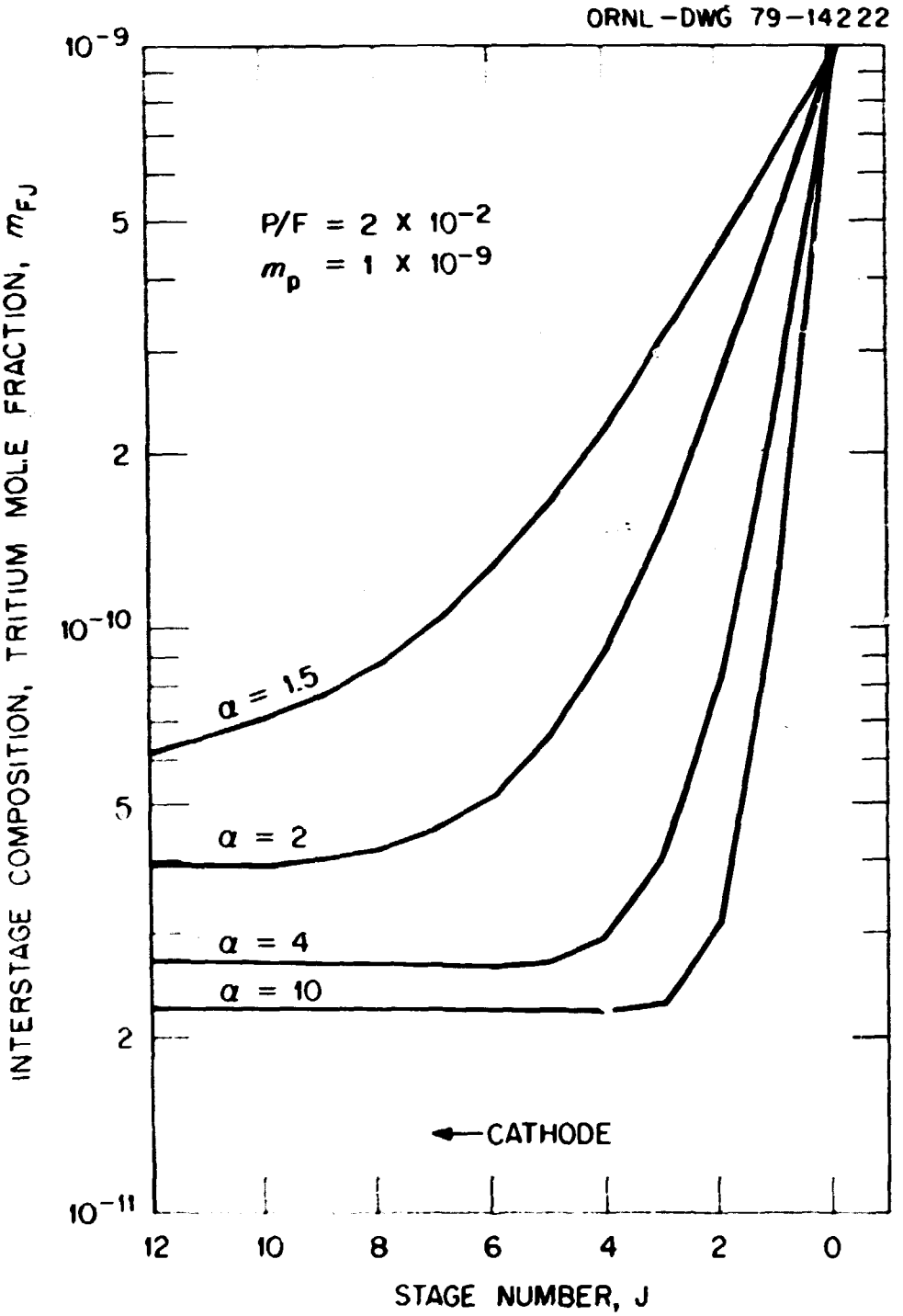

Figure 16. Interstage composition variation with respect to changes in separation factor for a constant P/F ratio.

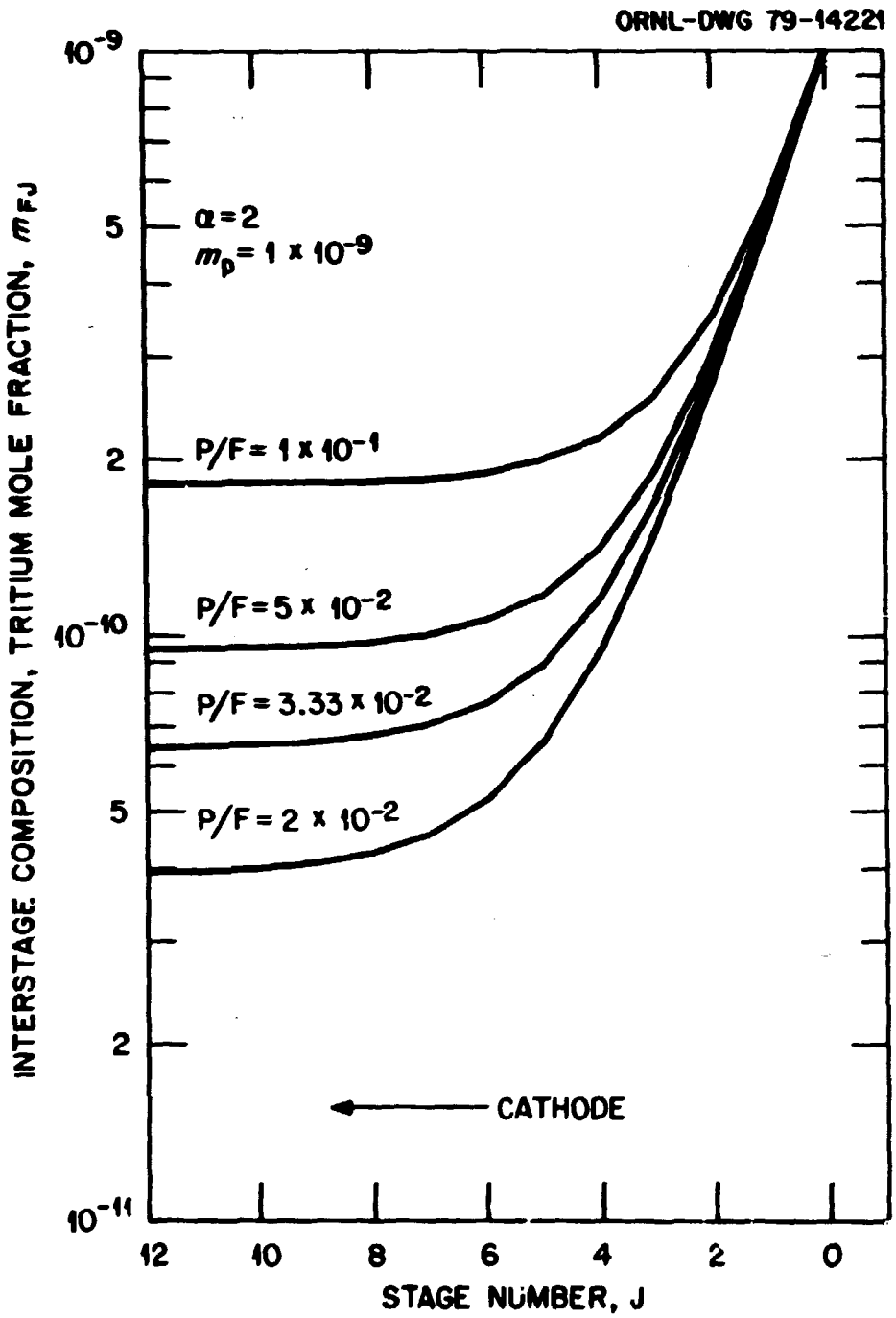

Figure 17. Interstage composition variation with respect to P/F ratios for a constant separation factor in the range expected for deuterium-tritium.

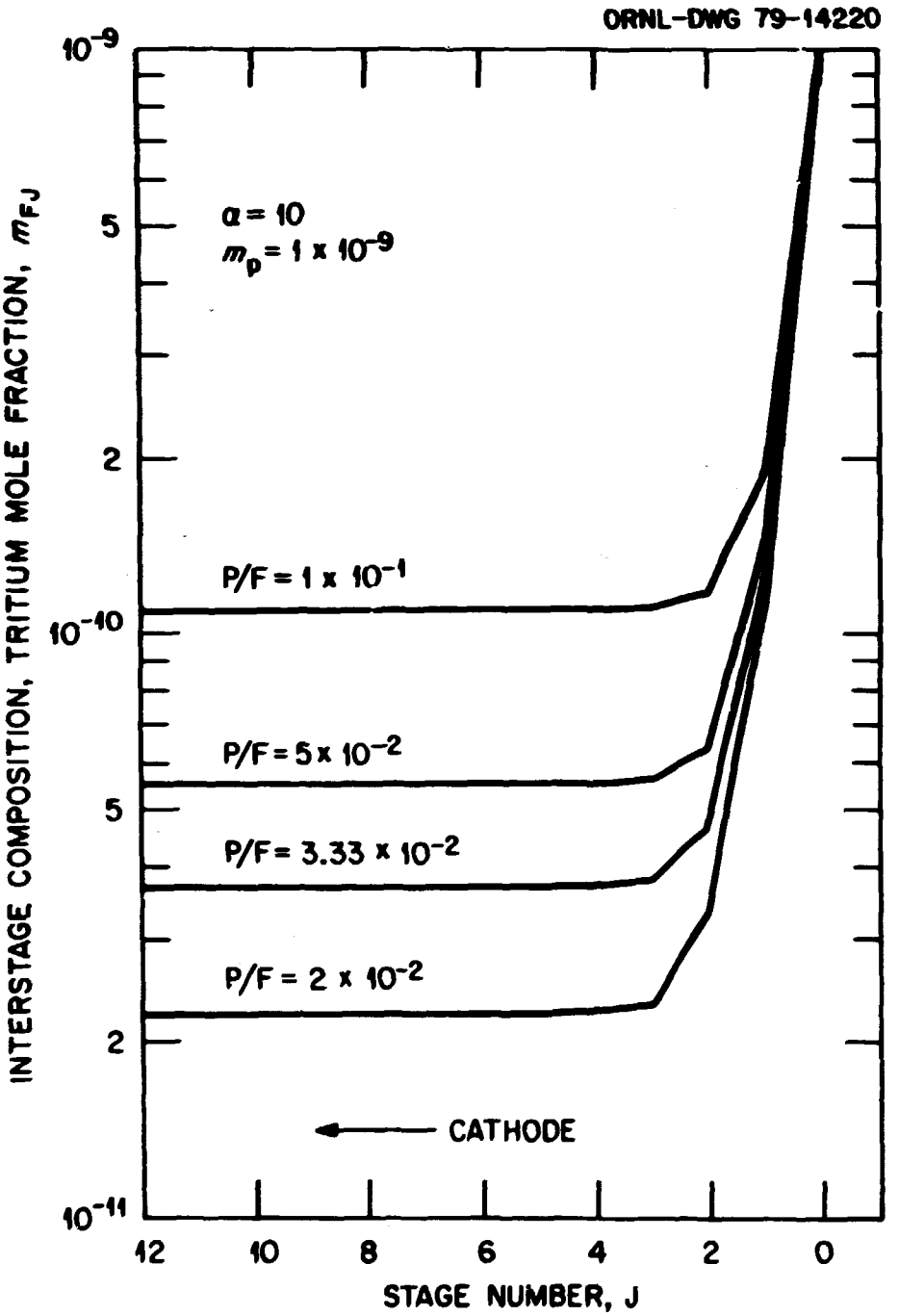

Figure 18. Interstage composition variation with respect to P/F ratios for a constant separation factor in the range expected for protium-tritium.

Cascade theory dictates that an ideal separation cascade is tapered (43) from stage to stage (maximum cross section at the feed point). This size tapering is theoretically more efficient than a square cascade because total cascade volume and energy requirements are minimized. If a tapered cascade is not possible, its efficiency can be approximated by a "squared-off" tapered cascade consisting of a series of square cascade sections of diminishing size (from the feed point) connected in a series arrangement. Designing such a squared-off tapered cascade can be accomplished by using the expression for the enrichment factor for each square section of the taper (Equation 22) along with simple material and heavy isotope balance relationships.

Experimental Results And Discussion

Several laboratory experiments have been performed in small multi-bipolar cells operating continuously with a steady supply of NaOH-containing feed and a continuous product removal. In a typical multi-bipolar cell experiment, the cell is initially filled with feed of the same tritium concentration as would be fed to the cell during the duration of the experiment. The multibipolar cell was then operated at constant current until steady state conditions were obtained (i.e., a constant tritium activity in the product stream is achieved). One such experiment was performed with the following cell parameters: five separation stages (four bipolar electrodes plus the terminal cathode), electrodes with an area of 6.0 cm^2 each, and 0.3 A cm^{-2} current density. This multistage system was fed with 3.3 N NaOH to the cathode compartment at a rate of 1.105 moles H_2/day (19.43 ml/day of 3.3 N NaOH) and had a P/F = 0.2268. The tritium

content in the feed was 4.747 μCi/mole H_2. This multistage system was operated for a total of 24 days, 8 days of which were at steady state. Cell temperature was maintained at an average of 85 ± 5°C by circulating 65°C water through heat exchanger tubes in the cell body.

The single stage separation factor for the above-described experiment was found by a trial-and-error solution of Equation (22). The separation factor per stage for protium-tritium was calculated to be $\alpha_{HT} = 6.3$. At the end of this experiment, samples were taken from each interstage compartment and analyzed for tritium. Figure 19 gives the measured concentration profile through the cascade for this particular experiment. It can be seen from Fig. 19 that the experimentally observed tritium concentration between individual stages (circles) closely followed that predicted by Equation (22). Note that nearly all enrichment has taken place in the first two stages. The other three stages would have been better utilized if a smaller P/F ratio could have been used. However, without a means of continuously removing electrolyte from the anode compartment, the P/F ratio was limited to a relatively high value. The sodium hydroxide normality in the anode compartment (N_P) was governed by the feed normality (N_F) and by the P/F ratio [i.e., $N_P = N_F/(P/F)$].

Further experimental evaluations were made with a larger electrode area (26.4 cm^2 each) multistage system. This system contained three separation stages (2 bipolar electrodes) and was operated with a current density of 0.3 A cm^{-2}. A continuous electrolyte removal system was attached to the anode compartment of this larger system; addition of the electrolyte removal system resulted in a slightly longer time needed to reach (as compared to the earlier experiment) steady state conditions because of the additional effective volume of the anode compartment (30%

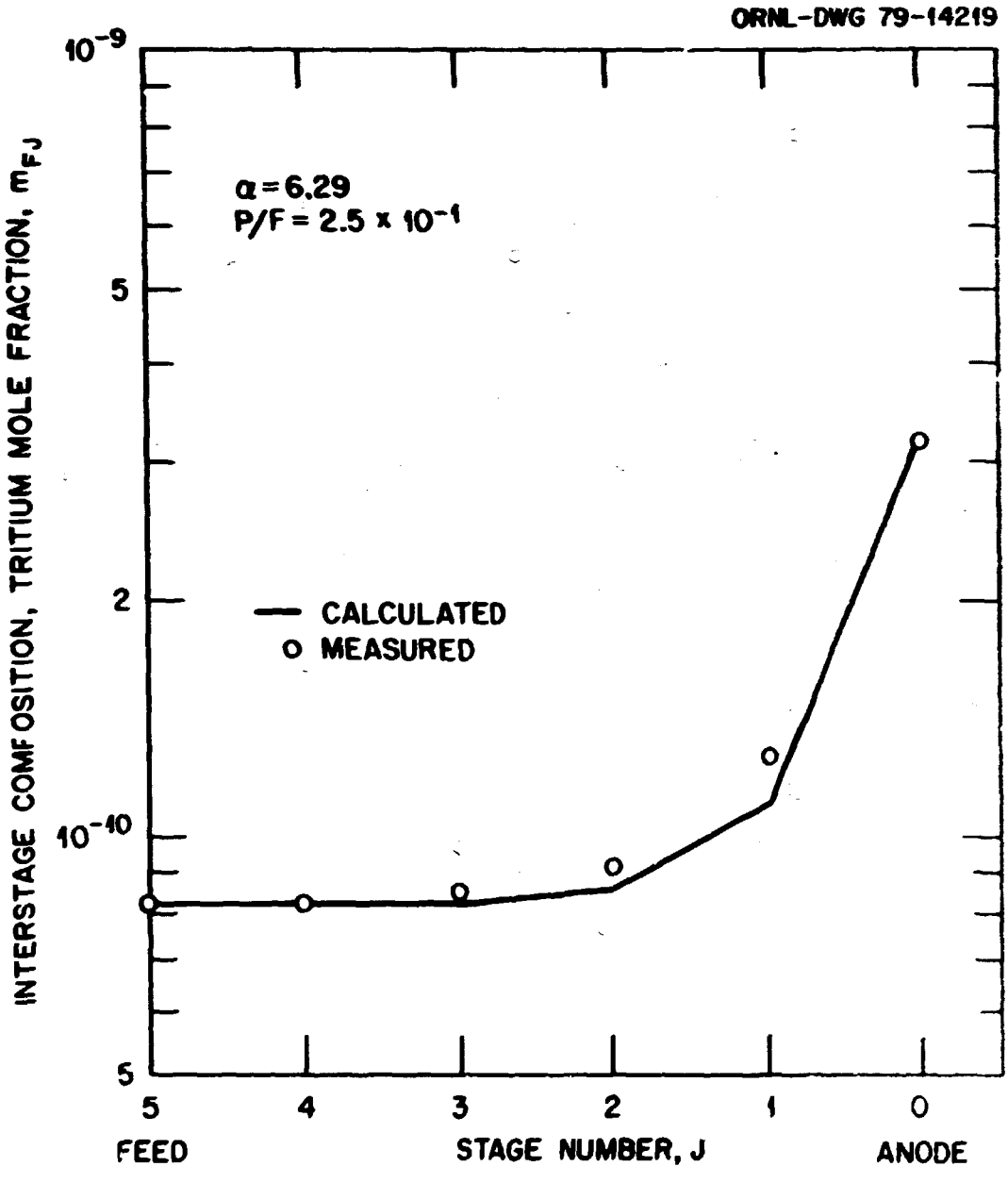

Figure 19. Interstage composition for a multistage experiment without an electrolyte removal system.

increase for this particular system). However, this same electrolyte removal system, as described, could accommodate a multistage system approximately 25 times larger than the one to which it was applied, and thus would not result in a significant increase in the anode volume and NaOH concentration.

With the larger multistage system, the cell was filled with 6.7 N NaOH which had a tritium concentration of 6.98 μCi/mole H_2. The system was then operated at 0.3 A cm^{-2} current density and tritiated water of the same NaOH and tritium content was fed to the cathode compartment. The feed rate was 3.54 moles H_2/day (62.6 ml/day of 6.7 N NaOH) with an average cell temperature of 88.5 $\pm$2°C. To hasten the rate of increase in tritium concentration in the multistage system, no product was withdrawn during the initial part of the experiment except for 0.5 ml/day necessary for analytical purposes. In 49 days of operation the anode compartment reached a maximum tritium activity of 77.76 μCi/mole H_2 (an enrichment of 11.14 times the feed concentration). At this point in time the system was forced to a steady state condition by withdrawing more product (5.2 ml/day) and at the same time increasing the feed rate by the amount being withdrawn (feed rate increased to 67.8 ml/day).

The system was operated for 8 days under these conditions to assure steady state composition throughout the cascade. The waste stream (stream depleted in tritium) tritium concentration during the entire experiment was 1.18 μCi/mole H_2 which yields a total separation factor between the product and waste streams of 65.9. Using the tritium concentrations at steady state, Equation (22) was solved by trial and error to determine the protium-tritium separation factor; this solution gave an α_{HT} = 6.9

for the single stage separation factor. At the end of the experiment, samples were taken from each interstage compartment and analyzed for tritium; Fig. 20 shows the measured concentration profile through the cascade. Once again the experimentally observed tritium concentration between individual stages closely followed that predicted by Equation (22). Note in Fig. 20 the more efficient utilization of all stages. This is a direct result of the lower P/F ratio (7.58×10^{-2}) as compared to the previous multistage experiment (see Fig. 19).

Conclusions

Single bipolar cell experiments have indicated that at 90°C the protium-tritium separation factor, α_{HT}, should be 11. In the multistage experiments, the single stage separation factors were found to be 6.3 and 6.9 as compared with about 8.0 for regular electrolysis. No definitive reason for these lower separation factors can be given at this time. Possible reasons could include loss of tritium by evaporation or cell leakage.

Two multistage cascade experiments with countercurrent electrolyte flow established that Equation (22) is an adequate mathematical model for isotope separation by bipolar electrolysis since the measured concentration gradient throughout the cascade agrees well with calculated values. Future multistage experiments with countercurrent electrolyte flow should include larger cells which would better facilitate the use of necessary auxiliary systems (e.g., electrolyte removal) and improve the temperature control throughout the system. It is evident that bipolar electrolytic separation of hydrogen isotopes is a viable concept but requires further experimental study to determine its economic and engineering feasibility.

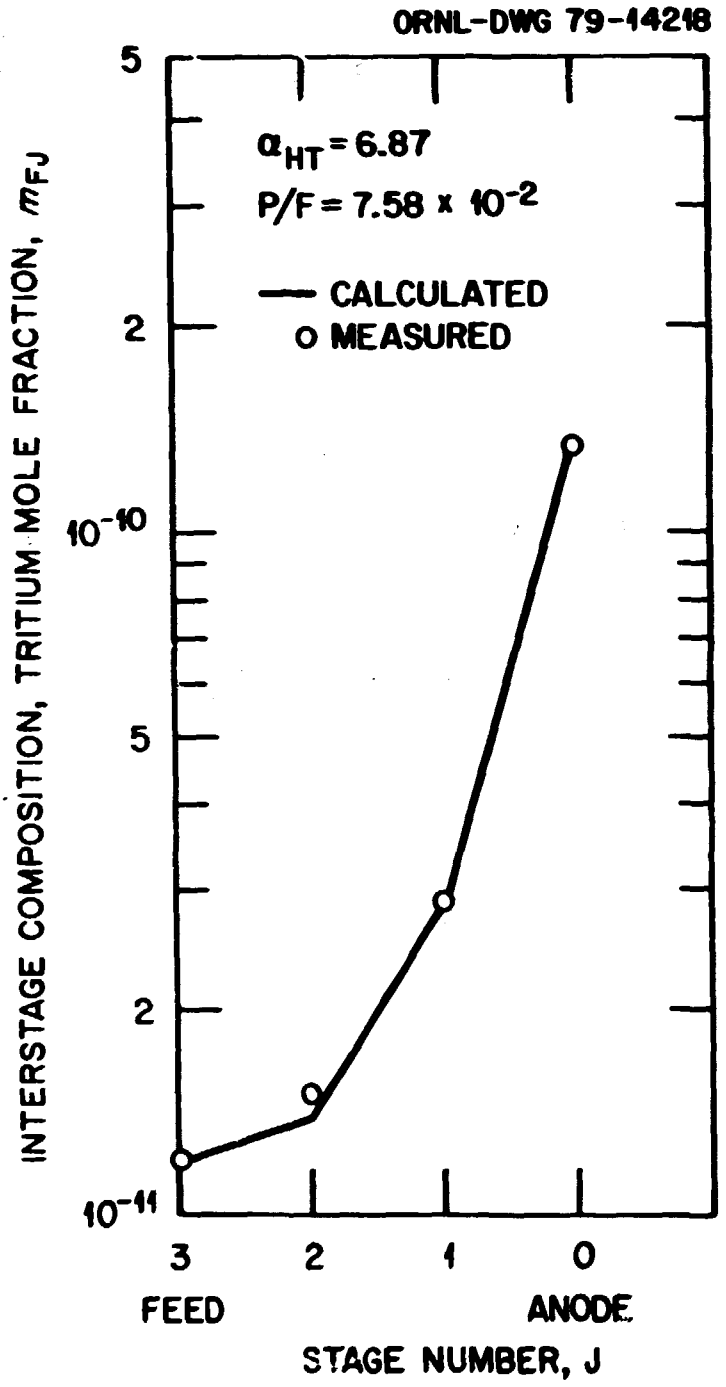

Figure 20. Interstage composition for a multistage experiment with an electrolyte removal system.

ELECTROLYTE MAINTENANCE

Introduction

The operation of a bipolar cascade requires ancillary processes for the maintenance of the desired concentration of electrolyte throughout the system. Electrolyte must be added to the primary aqueous feed stream at the head of the cascade, and excess electrolyte in the terminal anode compartment, being concentrated as a result of dissociation of water, must be removed. If the excess electrolyte is not removed from the anolyte, the concentration in the anode compartment would increase to an equilibrium value which is proportional to the feed concentration by the factor F/P, where F and P are the volumetric flow rates of the aqueous feed and product streams, respectively. At present, sodium hydroxide serves as the electrolyte for the bipolar process, but potassium hydroxide has been considered as an alternative and may be preferred under some operating conditions.

Several possibilities have been evaluated for cascade electrolyte maintenance. The most suitable processes appear to be electrodialysis for preparation of the caustic feed solution and conversion of hydroxide to carbonate followed by water evaporation for the removal of excess electrolyte in the terminal anode compartment. Condensed water vapor from this latter process is returned to the terminal anode compartment.

Electrolyte Preparation

Electrodialysis cells utilizing cation exchange membranes, such as NAFION*, are currently being operated for the commercial production of

---

*Registered trademark of E. I. duPont deNemours & Co. (Inc.) for its perfluorosulfonic acid products.

caustic from salt brines (42-49). This technology can readily be applied to the preparation of electrolyte feed solution for the bipolar electrolysis cascade.

The principles of electrodialysis are schematically represented in Fig. 21 for the production of sodium hydroxide from concentrated salt solutions. The cation exchange membrane, which separates the caustic catholyte from the anolyte, is selectively permeable to excess sodium cations (Na^+) resulting from the oxidation reaction at the anode, but rejects most hydroxyl ions (OH^-) formed by the reduction of hydrogen at the cathode. Therefore, most of the current is carried by sodium cation transfer through the membrane which then combines with hydroxyl ions to form product caustic.

The efficiency of the dialysis cell is determined by the percentage of hydroxyl ions remaining in the catholyte to form caustic. If the efficiency were 100%, the production of one mole of NaOH would require 26.8 A-hours. An efficiency of 80% is typical in a cell producing 30% NaOH solution at a current density of 0.3 A cm^{-2}. Efficiency and cell voltage vary with membrane composition, temperature, current density, and solution compositions (47, 48, 52, 53).

Experimentally, "deuteroxide" (NaOD) solutions with concentrations up to 25% have been prepared from solutions of Na_2CO_3 in D_2O using small test cells with NAFION membranes. These solutions were produced in batches for subsequent experimentation to determine D-T separation factors in single bipolar electrolysis cells, but continuous operation for direct feed to a cascade should be achievable, but engineering development is required.

ORNL-DWG 79-11524R2

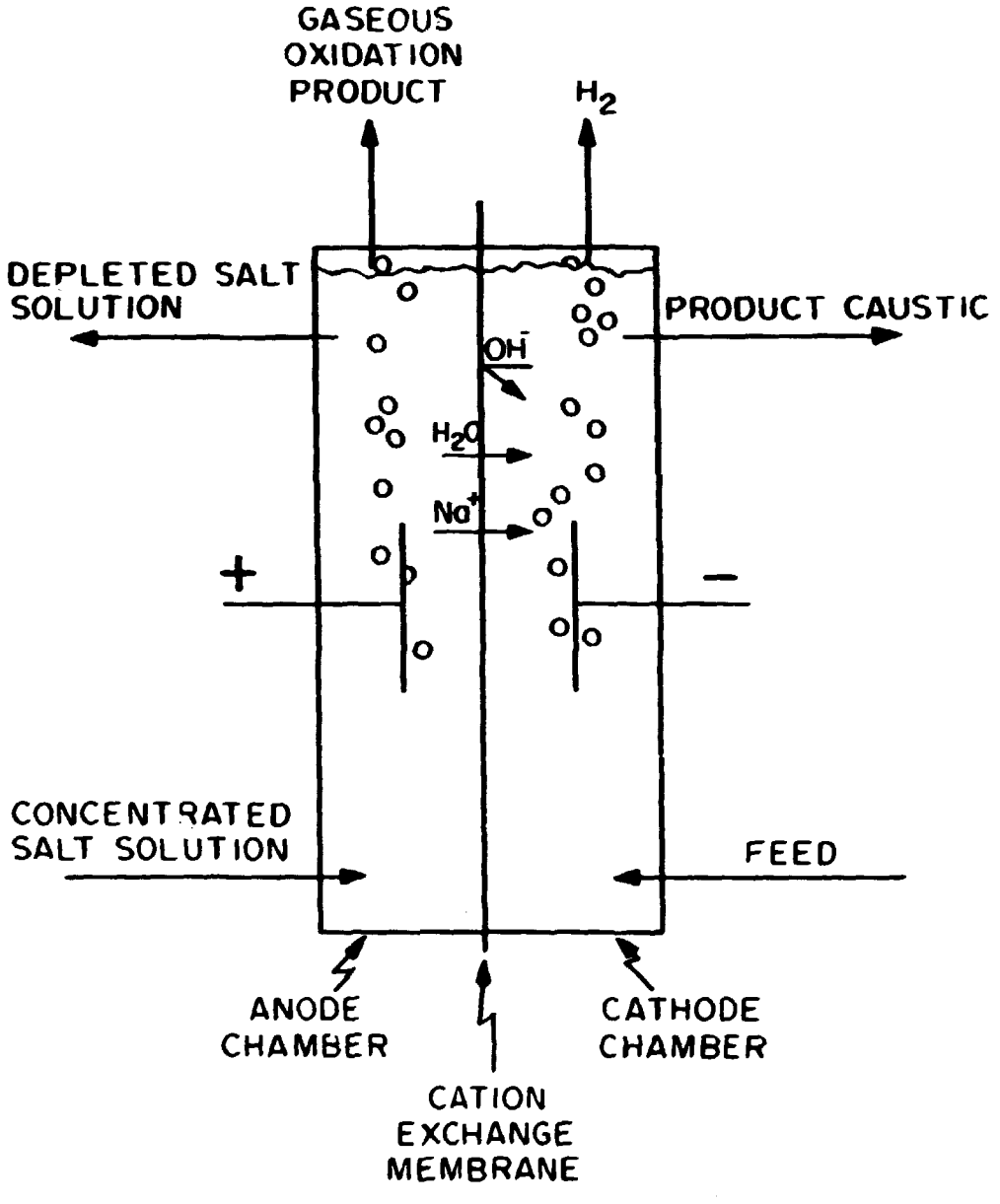

Figure 21. Schematic representation of the electrodialysis process.

Electrolyte Removal

In order to maintain a uniform concentration of sodium hydroxide throughout the bipolar electrolytic cascade, a quantity of electrolyte must be removed from the terminal anode compartments at a rate proportional to the rate of water electrolysis.

Electrodialysis was originally considered a feasible method for the direct transfer of sodium from the electrolyte solution in the terminal anode compartment of the cascade back to the feed stream. This direct transfer method was rejected, however, because of excessive water migration through the membrane which impaired the separative efficiency of the cascade. However, for a feed preparation process disjoint from contact with the anolyte of the cell, water migration is not a deleterious factor since the water source is the same as that used for the caustic catholyte product.

Alternately, the removal of sodium from an aqueous hydroxide solution can be achieved by reaction with CO_2 to form sodium carbonate, and subsequent evaporation of the water, leaving the sodium behind as dry carbonate (Na_2CO_3) (53). During one experiment with a bipolar cascade, an electrolyte stream was withdrawn from the anode compartment for the purpose of removing sodium by this process. The flow rate of this recycle stream was made equivalent to the rate of water electrolysis, i.e., the W stream of the cascade.

Possible reaction products of sodium hydroxide with CO_2 are anhydrous or hydrated sodium carbonate and sodium bicarbonate according to the equation

$$NaOH_{(aq)} + CO_2 \rightarrow Na_2CO_3 \cdot X(H_2O) + NaHCO_3 \cdot Y(H_2O).$$

Evaporation at elevated temperatures yields anhydrous crystals, and above 270°C, sodium bicarbonate decomposes to form anhydrous sodium carbonate by the reaction

$$2NaHCO_{3(s)} \rightarrow Na_2CO_{3(s)} + H_2O_{(g)} + CO_{2(g)},$$

so that theoretically all of the hydrogen isotopes can be recovered as water for recycling. This sodium removal technique is particularly well suited for application to the bipolar cascade separation of tritium since no hydrogen isotopes are removed from the system as a result of the electrolyte maintenance process.

The recovered carbonate may be used for the electrodialytic production of hydroxide solution for feed to the cascade so that the sodium remains in a closed process loop, or a portion of it may be discarded to remove concentrated impurities from the system if this becomes necessary.

A spray-drying unit appeared to be a suitable approach for the continuous removal of sodium (54). Aqueous hydroxide is atomized in a stream of CO_2 and heated to yield a gaseous effluent of water vapor, excess CO_2 and a solid product of dry carbonate powder. A small spray reactor was operated discontinuously in the laboratory in conjunction with trial experiments of the bipolar cascade test cell (described earlier) to demonstrate the applicability of the technique. Results were generally satisfactory with an achieved conversion to carbonate of up to 99%. For the bench-scale bipolar cascade cell, a small apparatus for the continuous removal of excess sodium from the terminal anode compartment was assembled and successfully operated for the duration of the experiment. The system in its final configuration is schematically shown in Fig. 22.

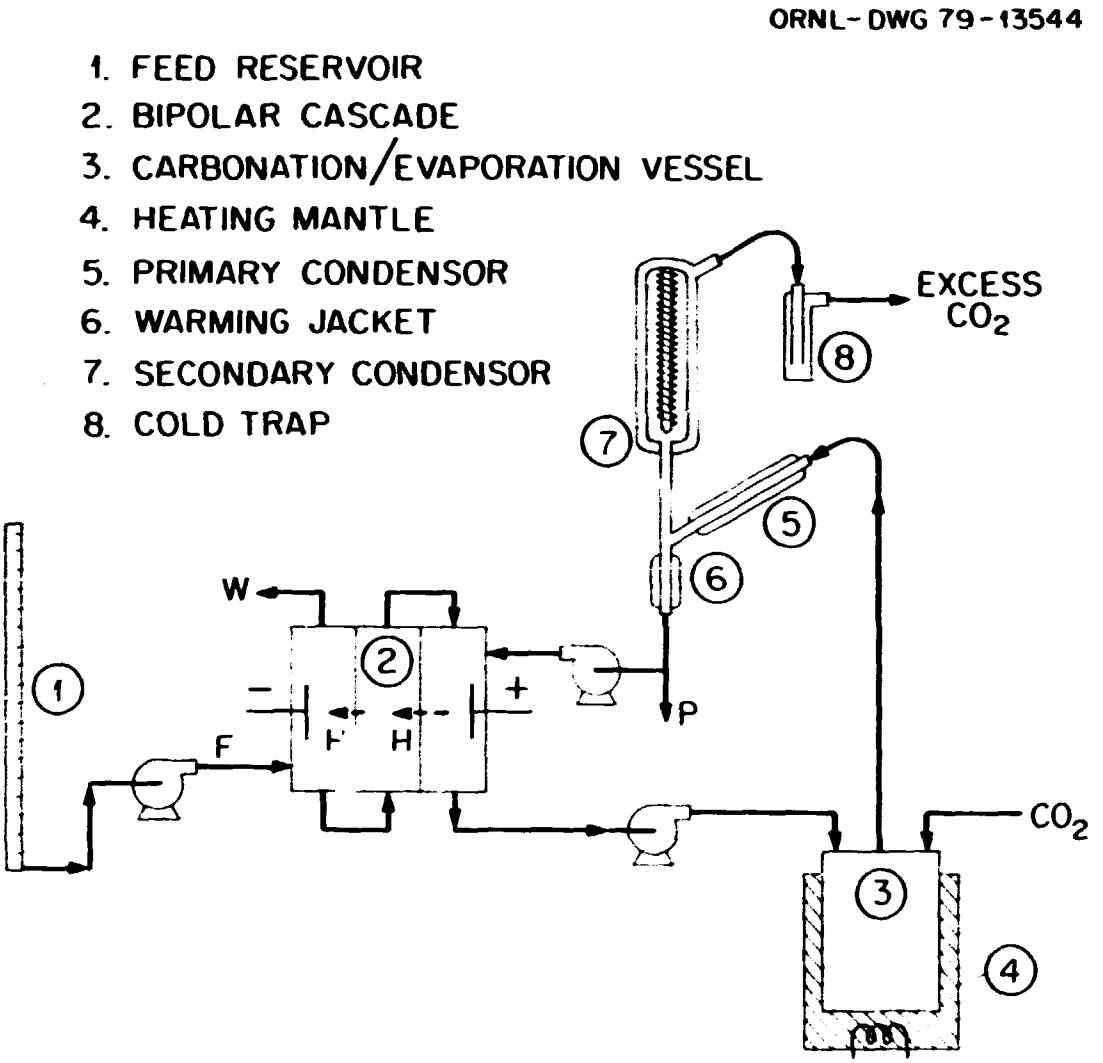

Figure 22. Schematic representation of the experimental sodium removal system.

Aqueous electrolyte was pumped from the terminal anode compartment of the cell (2) to a carbonation/evaporation reactor (3), which was externally heated by an electric mantle (4). Carbon dioxide was introduced into the reactor and water vapor extracted. As the water vapor and excess CO_2 passed through the primary condenser, most of the water was condensed and collected in a reservoir (6), which was heated to about 70°C to minimize the amount of dissolved CO_2 in the recycle water and product stream.

Gas and residual water vapor passed through the vertical branch of the manifold to a high-speed condenser (7), where most of the remaining water was condensed. Finally, gas proceeded into a cold trap (8) to freeze out any residual water being carried by the CO_2 stream. The ice which collected in the cold trap was occasionally melted and returned to the reservoir.

The carbonation/evaporation reactor did not employ the spraying mode of operation, as conceptualized, but instead the aqueous electrolyte dripped into a vessel in which a CO_2 atmosphere was maintained. The average aqueous flow rate was about 3 ml/hr and that of the entering CO_2 stream was 200 sccm. Reactor temperature was maintained at 350°C. Almost all of the water vapor was recovered in the primary and secondary condensers, with less than 1% of the total flow reaching the cold trap. After one month of operation, a sample of the solid residue collected in the reactor was analyzed and determined to be completely converted to anhydrous sodium carbonate (Na_2CO_3).

One disadvantage of this sodium removal system was the addition of about 30 ml to the effective anode compartment volume of the bipolar cascade test cell, which had the effect of increasing the time required

for attainment of a steady state equilibrium within the cell. However, this system was capable of handling approximately twenty-five times the sodium removal rate required in this experiment; as the cascade size increases, the relative volumetric contribution to the anode compartment by the sodium removal system would decrease.

Conclusions

Electrodialysis appears to be an effective method for the preparation of aqueous hydroxide feed solution for the bipolar cascade without significantly alterating the isotopic distribution. Anolyte hydroxide concentration can be maintained by reacting the aqueous hydroxide with CO_2 and subsequently evaporating the water for recycle to the anode compartment, leaving excess sodium behind as anhydrous carbonate (Na_2CO_3). Engineering scale-up of both of these processes should be in the realm of existing technology, and, unless impurities interfere with cell efficiency, would permit recycle of sodium in the system, thus avoiding large build-up of waste electrolyte. Impurity concentrations can probably be controlled by discarding part of the sodium carbonate.

SUMMARY

The present status of the hydrogen isotope separation process using bipolar electrolysis with countercurrent electrolyte flow indicates that the electrode material requirements are sufficiently met by using the Pd-25% Ag alloy foil. However, other electrode materials should be investigated with the goals of lowering the electrode cost and reduction of overvoltage. The measured value of separation factor, α_{DT}, using the

Pd-25% Ag bipolar electrode is sufficient to permit tritium removal from D_2O. The discrepancy in the protium-tritium separation factor as determined from the two multibipolar electrode experiments with that measured in single cell experiments (6.3 and 6.9 versus 11 respectively) requires investigation.

The small temperature dependence of the deuterium-tritium separation factor and the lack of any dependence on current density is a very important positive feature of the bipolar electrode. Experiments to determine the protium-tritium and protium-deuterium separation factor dependence on temperature and current density need to be conducted to verify the postulation that these isotope pairs exhibit a similar behavior to that of deuterium-tritium. Current density of 0.3 A cm^{-2} has been achieved in a continuous mode, and 0.5 A cm^{-2} should be possible for future continuously-fed systems of larger scale. Although, in the above described multibipolar electrode experiments, heat was added to the cell in order to maintain a constant temperature, heat addition or removal associcted with a higher current density (>0.3 A cm^{-2}) and/or larger area cells will require further study.

Methods of fabrication and assembly of large area thin mosaic electrodes also need to be developed. The estimated power consumption for BPE isotope separation seems suitable for an economic process. The present status of power consumption for normal electrolysis and for the bipolar process is summarized in Figure 23 (55). The "future goal" line essentially represents the present performance of the Solid Polymer Electrolyte process developed by General Electric Company. However, this process exhibits a very low hydrogen isotope separation efficiency

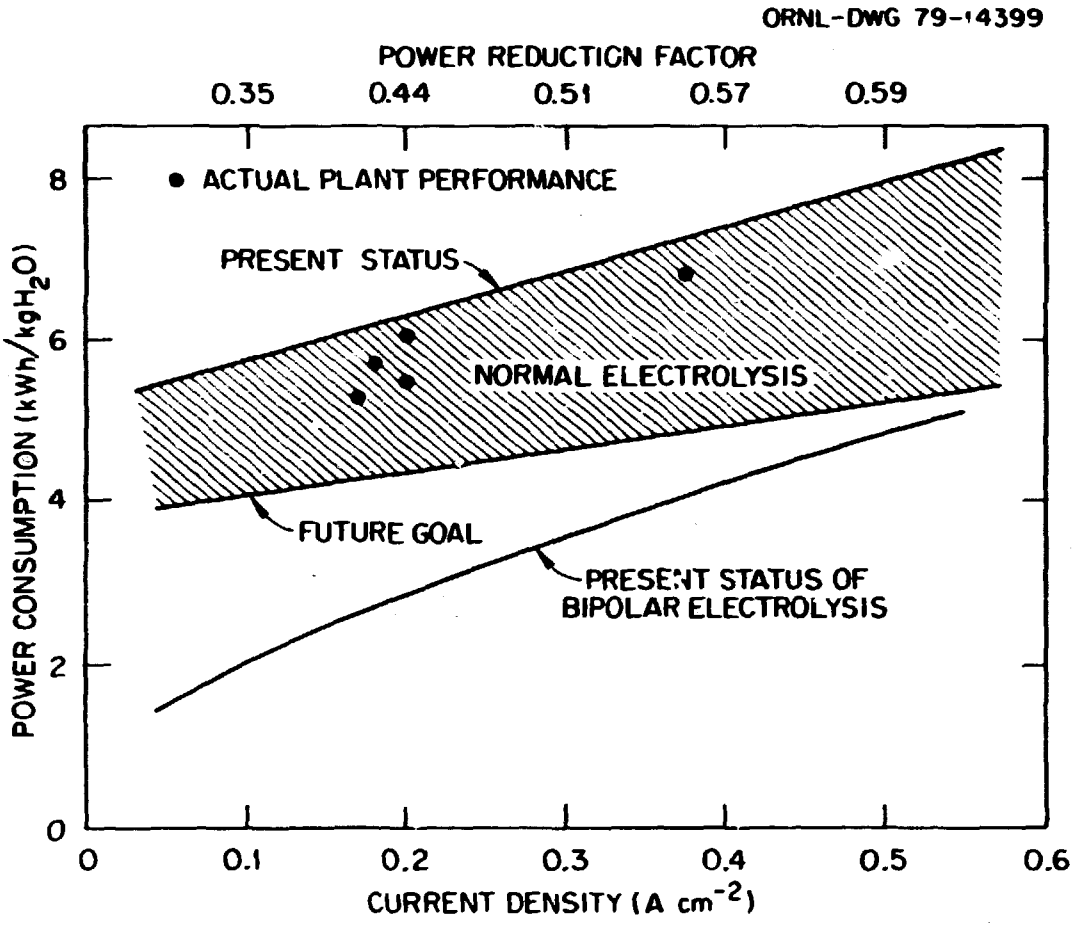

Figure 23. Comparison of power consumption in normal electrolysis with that of a bipolar Pd-25% Ag electrode. The power required to electrolyze 1 kg of water in normal electrolysis is shown using data from References 28-31 and 55. The line for power consumption in bipolar electrolysis is calculated for an amount of hydrogen equivalent to 1 kg of water when transferred through the bipolar electrode from one compartment to the next one.

(α_{HD} = 1.6) (56). Further research on power consumption needs to be done to yield more quantitative long-term evaluation. More detailed studies are needed to understand the individual processes occurring during hydrogen reduction, permeation and reoxidation at the bipolar membrane so as to reduce the voltage drop through the electrode to a minimum.

Technology associated with electrolyte removal from the terminal anode compartment, which has been investigated only in a preliminary manner, requires development of an automated system and a suitable method of attachment to the terminal anode compartment so as to form an integral part of a large-area electrode, multistage system. Construction of a physically larger cell would permit more suitable study of this problem. Feed pretreatment with respect to the removal of contaminants as well as what contaminants can be tolerated in the bipolar process require investigation.

Although studies necessary to establish complete scientific understanding of the many aspects of bipolar electrolysis are, at present, insufficient, the information that has been obtained indicates that the concepts are sound. The operation of multibipolar cells, under a limited range of conditions, shows unequivocally that he process is viable.

REFERENCES

1. O. N. Salmon, "The Electrolytic Separation of Hydrogen Isotopes by Migration Through a Palladium Membrane." KAPL-1272, June 25, 1956.

2. F. T. Barr and W. P. Drews, "The Future for Cheap Heavy Water," Chem. Eng. Progress, 56 (1960)49.

3. D. M. Drazic, Progress Report to E.P.A. from the Faculty of Technology, University of Belgrade, Belgrade, Yugoslavia, Jan.-Dec.1973.

4. S. V. Ribnikar and J. D. Pupezin, "Possibilities of Tritium Removal from Waste Waters of Pressurized Water Reactors and Fuel Reprocessing Plants", presented at the 13th A.E.C. Air Cleaning Conference, San Francisco, Califoria, 1974.

5. F. A. Lewis, "The Palladium Hydrogen System", Academic Press 1967.

6. E. Wicke and G. Bohmholdt, "Hydrogen Diffusion Through Pd and Pd/Ag Hydrides at High Hydrogen Content". Ztschr. f. Phys. Chem. N. F. 42 (1964) 115.

7. A. Kussner and E. Wicke, "Palladium Membrane as a Hydrogen Diffusion Anode." Ztschr. f. Phys. Chem. 24 (1960) 152.

8. W. Wicke and H. G. Nernst, "The Phase Diagram and Thermodynamic Relations in the System Pd/H_2 and Pd/D_2 at Normal Temperatures; H/D - Separation Effect." Ber. Bunsenges. Phys. Chem. 68 (164) 224.

9. M. A. Devanathan and Z. Stachurski, "The Adsorption and Diffusion of Electrolytic Hydrogen in Palladium", Proc. Roy. Soc. London, A270 (1962) 90.

10. M. von Stackelberg and P. Ludwig, "Diffusion of Hydrogen through Palladium-Hydrogen", Z. Naturf. 19a (1964) 93.

11. P. Damour and G. Castellan, "The Transmission of Hydrogen through a Palladium Membrane Electrode III. Pressure and Temperature Dependence." J. Electrochem. Soc. 111 (1964) 1280.

12. J. B. Hunter, "Ultra Pure Hydrogen by Diffusion Through Palladium Alloys", Amer. Chem. Soc., Div. Petrol. Chem., 8 (1963) B49.

13. P. S. Perminov, A. A. Orlov, and A. N. Frumkin, "The Effect of Pressure on the Solubility of Molecular Hydrogen in the β-phase of the Palladium-Hydrogen System". Doklady Acad. Nauk. S.S.S.R., 84 (1952) 749.

14. H. Brodowsky, H. Gibmeyer and E. Wicke, "The H/D Separation Factors in Electrolysis and Diffusion using Pd and Pd/Ag Membranes", Ztschr. f. Phys. Chem. N. F. 49 (1966)222.

15. J. B. Hunter, U. S. Patent 2,773,561, 1955.

16. H. Brodowsky and E. Poeschel, "Hydrogen in Palladium-Silver Alloys", Ztschr. f. Phys. Chem. N. F. 44 (1965) 143.

17. A. Kussner, "Electrolytic Measurement of Hydrogen Diffusion in Homogenous Palladium-Silver-Hydrogen Alloys", Ztschr. f. Phys. Chem. N. F. 36 (1963) 383.

18. E. Wicke and G. Holleck, "Diffusion Coefficients of H and D in Pd/Ag Foil Electrodes at High Hydrogen Content by Measuring the Hydrogen Overvoltage", Ztschr. f. Phys. Chem. N.F. 46 (1965) 123.

19. E. J. Serfass, "Activated Surfaces Useful in the Production of Hydrogen", U. S. Patent 3,448,035, 1966.

20. D. T. Sawyer and D. L. Roberts: "Experimental Electrochemistry for Chemists", J. Wiley, 1974, p. 302.

21. J. O'M. Bockris and A. K. N. Reddy, "Modern Electrochemistry", Plenum Press, 1977, p. 1363.

22. M. Pourbaix, "Atlas of Electrochemical Equilibria in Aqueous Solutions," Pergamon Press, 1966, p. 360.

23. I. N. Maksimova and V. F. Yushkevich, "Electrical Conductivity of Sodium Hydroxide Solutions at High Temperatures", Russian J. Phys. Chem. 37 (1963) 475.

24. V. F. Yushkevich, I. N. Maksimova and V. G. Bullan, "Electric Conductivity of KOH Solutions at High Temperatures", Soviet Electrochemistry 3 (1967) 1342.

25. K. J. Vetter, "Electrochemical Kinetics", Academic Press, N. Y. 1967, p. 9.

26. A. M. Polcaro, P. F. Ricci, and A. Viola, "The Electrochemical Behavior of a Palladium-Silver (Hydrogen) Electrode", Ann. Chim. 66 (1976) 711.

27. J. P. Hoare and S. Schuldiner, "Mechanism of Hydrogen Producing Reactions on Palladium, IV. Electrochemical Kinetics of the α-Palladium-Hydrogen System in Acid Solutions". J. Electrochem. Soc. 104 (1957) 564.

28. H. Wuellenweber, J. Mueller, "Lurgi Pressure Electrolysis", Proceedings of the Symp. of Water Electrolysis, p. 1, Electrochem. Soc. Meeting, May 1978, Seattle, Washington.

29. M. D. Brown, "Brown Boveri Electrolyzers Today and in the Near Future", Ibid., p. 16.

30. K. Christiansen and T. Grundt, "Large Scale Hydrogen Production", Ibid., p. 24.

31. J. H. Russel, "Design and Development of Solid Polymer Electrolyte Water Electrolyzers for Large Scale Hydrogen Generation", Ibid., p. 77.

32. J. O'M. Bockris, "The Solar-Hydrogen Alternative", John Wiley, N. Y., 1977.

33. S. Kaufman and W. F. Libby, "The Natural Distribution of Tritium", Phys. Rev. 93 (1954) 1337.

34. J. Bigeleisen, "Correlation of Tritium and Deuterium Isotope Effects", Proceedings of the Int. Symp. on the Detection and Use of Tritium in the Physical and Biological Sciences. Vienna, May 1961, Vol. I, p. 161.

35. L. P. Roy, "Influence of Temperature on the Electrolytic Separation Factor of Hydrogen Isotopes", Can. J. Chem. 40 (1962) 1452.

36. B. S. Johnson, et al., "Isotopic Purification of Tritium by Electrolysis", May 1958, DP 261.

37. H. V. Butlar, W. Vielstich and H. Barth, "Deuterium and Tritium Separation Factors During Electrolytic Hydrogen Evolution", Ber. Bunsenges. 67 (1963) 650.

38. J. O M. Bockris and D. F. A. Koch, "Comparative Rates of the Electrolytic Evolution of Hydrogen and Deuterium on Iron, Tungsten, and Platinum". J. Phys. Chem. 65 (1961) 1941.

39. B. E. Conway, "Kinetics of Electrolytic Hydrogen and Deuterium Evolution". Proc. Roy. Soc. A256 (1960) 128.

40. G. P. Lewis and P. Ruetschi, "The Dependence of the Electrolytic Hydrogen-Deuterium Separation Factor on the Electrode Potential", J. Phys. Chem. 66 (1962) 1487.

41. A. E. Brodsky, "Isotopenchemie", Akademie Verlag, Berlin, 1961, p. 62.

42. M. Hammerli, W. H. Stevens and J. P. Butler, "C.E.C.E. Process for Hydrogen Isotope Separation", from "Separation of Hydrogen Isotopes", Ed. H. K. Rae, American Chemical Society, Symposium Series 68 (1978). p. 110.

43. H. R. C. Pratt, "Countercurrent Separation Processes", Elsevier Publishing Co., 1967.

44. G. E. Munn, "Nafion* Membranes-Factors Controlling Performance in the Electrolysis of Salt Solutions", presented at The Electrochemical Society Fall Meeting, October 1977, Atlanta, Ga.

45. T. Berzins, "Electrochemical Characterization of Nafion* Perflourosulfonic Acid Membranes in Chlor-Alkali Cells", ibid.

46. T. D. Gierke, "Ionic Clustering in Nafion* Perfluorosulfonic Acid Membranes and Its Relationship to Hydroxyl Rejection and Chlor-Alkali Current Efficiency", ibid.

47. A. J. Hopfinger, K. A. Mauritz and C. J. Hora, "Prediction of the Molecular Structure of Nafion* Under Different Physicochemical Conditions", ibid.

48. S. F. Burkhardt, "Radioactive Tracer Measurement of Sodium Transport Efficiency in Membrane Cells", ibid.

49. C. J. Hora and D. E. Maloney, "Nafion* Membranes Structured for High Efficiency Chlor-Alkali Cells", ibid.

50. C. J. Molnar and M. Dorio, "Effects of Brine Purity on Chlor-Alkali Membrane Cell Performance", ibid.

*Registered trademark of E. I. duPont deNemours & Co.(Inc.) for its perflourosulfonic acid products.

51. E. H. Price, "The Commercialization of Ion-Exchange Membranes to Produce Chlorine and Caustic Soda", ibid.

52. E. J. Peters and D. R. Pulver, "The Commercialization of Membrane Cells to Produce Chlorine and Caustic Soda", ibid.

53. Thorpe's Dictionary of Applied Chemistry, Fourth Edition, Longmans, Green and Co., N. Y., 1952.

54. J. E. Loeffler, Jr., R. A. Springer and E. L. Bolick (to Diamond Alkali Co.), Brit. 930, 931, U. S. 3,202,477, Alkali Metal Carbonate Manufacture.

55. P. W. T. Lu and S. Srinivasan: "Advances in Water Electrolysis Technology with Emphasis on Use of the Solid Polymer Electrolyte". Journ. Appl. Electrochem., 9 (1979) 269.

56. E. R. Ellis, Monsanto Research Corp., Mound Laboratories, private communication.

---

*Registered trademark of E. I. duPont deNemours & Co. (Inc.) for its perfluorosulfonic acid products.

APPENDIX A

CALCULATION OF THE MAXIMUM CURRENT DENSITY AT THE BIPOLAR ELECTRODE

When a constant current is applied through a bipolar electrode, it can be assumed that a linear concentration gradient of protium will be established along the electrode thickness dimension when a steady state condition is attained. The maximum current density can be calculated under steady state conditions using Fick's first law:

$$\frac{dN}{dt} = \frac{I}{nF} = Dq \frac{dC^*}{dx} \qquad (A1)$$

$$m.c.d. = \frac{I}{q} = nFD \frac{dC_{max}}{X} \qquad (A2)$$

$$dC_{max} = C_{max} - C_o \qquad (A3)$$

where C_{max} is the saturation concentration of protium at the cathode surface and $C_o = 0$ at the anode surface of the bipolar electrode. When the electrode is made of Pd-25% Ag alloy, C_{max} can be found from data in Ref. 16 and the protium diffusion coefficient from Ref. 17.

---

*N = number of moles
t = time in seconds
I = current in amperes
n = number of electrons exchanged per molecule
F = faraday = 96500 coulombs per equivalent
D = diffusion coefficient in cm^2 sec^{-1}
q = cross section area in cm^2
C = concentration in mols cm^{-3}
x = thickness in the direction of diffusion in cm

Concentration of protium in the electrode should be expressed in moles cm^{-3} of the alloy, but the data in Ref. 16 are given in terms of moles H/moles M (metal). Therefore

[moles $\cdot$ cm^{-3}] = $1/a^3$ [unit $\cdot$ cm^{-3}] x 4 [atoms M/unit] x B [moles H/moles M] x 1/A [moles M/atoms M]** or C_H = 0.157 B [moles H cm^{-3}].

The m.c.d. values calculated for three different electrode thicknesses and temperatures from 30 to 90°C are given in Table IAi.

Table IAi

Maximum Current Density Values as a Function of Electrode Thickness and Temperature

Temperature (°C)	B (H/M)	C_H (mole $\cdot$ cm^{-3})	$D_H \times 10^6$ cm^2 sec^{-1}	m.c.d. (A cm^{-2}) Electrode Thickness $\times 10^{-3}$ (cm) 2.5	3.8	7.6
30	0.396	0.0418	0.383	0.609	0.406	0.20
40	0.388	0.0410	0.479	0.746	0.497	0.24
50	0.381	0.0403	0.619	0.947	0.631	0.31
60	0.371	0.0392	0.774	1.153	0.768	0.38
70	0.361	0.0381	0.95	1.377	0.918	0.45
80	0.352	0.0372	1.20	1.700	1.13	0.56
90	0.343	0.0362	1.62	2.230	1.49	0.74

**a = 3.975 Å lattice parameter (16)

4 = factor resulting from the face centered structure of Pd-25% Ag

B = concentration of protium expressed in moles H/moles M (16)

A = 6.023 x 10^{23} atoms $mole^{-1}$ (Avogadro's number)

APPENDIX B

SEPARATION FACTOR EQUATIONS

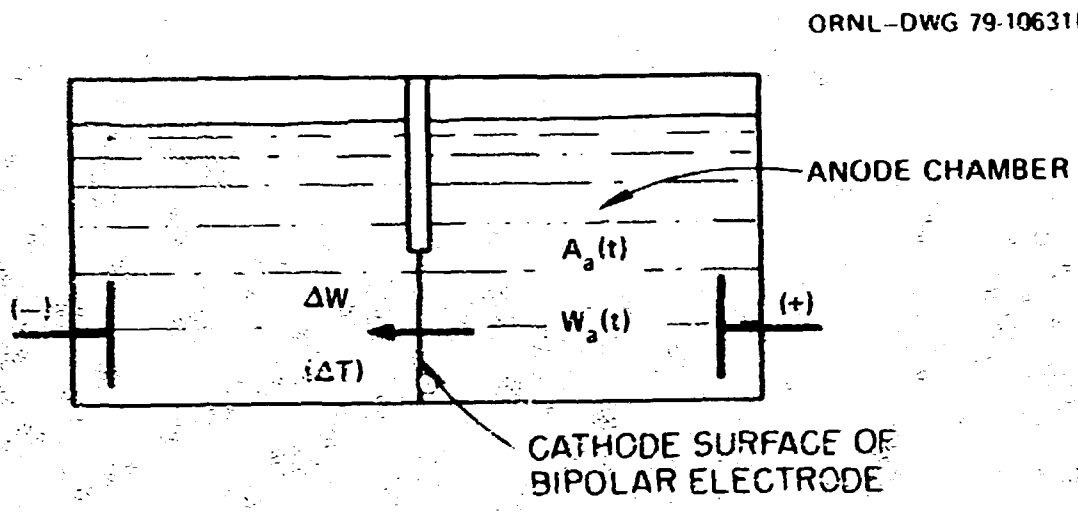

Figure B1. Variables associated with the anode chamber of a cell having a single bipolar electrode:

$W_a(t)$ = moles of hydrogen in anode chamber at time t,

$A_a(t)$ = curies of tritium per mole of hydrogen at time t,

ΔW = incremental molar quantity of hydrogen transported through the bipolar electrode,

ΔT = incremental molar quantity of tritium transported through the bipolar electrode.

Anode Chamber Analysis

Suppose at time t there are $W_a(t)$ moles of water in the anode chamber of a bipolar electrolysis cell, and assume the water consists of a binary mixture of either H_2O and T_2O or D_2O and T_2O with a tritium activity concentration of $A_a(t)$ curies of tritium per mole of hydrogen. At this same time, an incremental molar quantity of water is electrolyzed and the

hydrogen produced from this electrolysis (ΔW) is transported through the bipolar electrode to the adjacent cathode chamber. The tritium balance in the anode chamber then becomes

(tritium at time $t + \Delta t$) = (tritium at time t) − (tritium contained in increment ΔW)

or

$$T_a\,(t + \Delta t) = T_a\,(a) - \Delta T. \qquad \text{(B1)}$$

Further, assume that the incremental molar quantity which was transferred through the electrode has a tritium activity concentration, a(t), such that

$$a(t)\ \Delta W = \Delta T. \qquad \text{(B2)}$$

The separation factor for any binary isotope system can be defined as

$$\alpha = \frac{Y}{X} \quad \text{or} \quad \alpha = \frac{y/(1-y)}{x/(1-x)} \qquad \text{(B2a)}$$

where: Y = mole ratio of the light isotope to the heavy isotope in the new phase (i.e., through the bipolar electrode)

X = mole ratio of the light to the heavy isotope in the remaining phase (i.e., in the anode electrolyte)

y,x = mole fraction of the light isotope in the new and the remaining phases, respectively.

In terms of the heavier isotope mole fraction

$$y + n = 1 \longrightarrow y = 1 - n\ ,$$

$$x + m = 1 \longrightarrow x = 1 - m\ ,$$

where n and m are mole fractions of the heavier isotope in the new and the remaining phase, respectively. Substituting these values into Eq. (B2a) for y and x,

$$\alpha = \frac{(1-n)[1-(1-m)]}{(1-m)[1-(1-n)]} = \frac{m(1-n)}{n(1-m)}.$$

For low tritium mole concentrations[1], $(1-m) = (1-n)$ and $(1-n)/(1-m) \simeq 1$, and the separation factor may be expressed by the approximation

$$\alpha = m/n. \qquad \text{(B3)}$$

The mole fractions (m and n) for tritium are related to tritium activity concentration by a simple proportionality relationship:

$$A = km \longrightarrow m = A/k$$

$$a = kn \longrightarrow n = a/k$$

where k has the units of Ci tritium/mole tritium. Substituting these values in Eq. (B3) for m and n, we have

$$\alpha = \frac{A/k}{a/k} = A/a \text{ or } a = A/\alpha.$$

For the bipolar separative process, tritium activity concentration changes with time such that

$$a(t) = A(t)/\alpha. \qquad \text{(B4)}$$

Substituting Eq. (B4) into Eq. (B2) we have

$$A_s(t)\frac{\Delta W}{\alpha} = \Delta T.$$

---

[1]It can be shown that this simplifying assumption produces less than 1% error with a tritium content as large as 0.55 moles T_2O/L (0.01 mole fraction or 3.2×10^4 (Ci/mole of hydrogen).

Using this result for ΔT in Eq. (1), we have

$$T_a(t + \Delta t) = T_a(t) - A_a(t) \frac{\Delta W}{\alpha} .$$

Noting that in general $T_a(t) = A_a(t)\, W_a(t)$, we have

$$A_a(t + \Delta t)\, W_a(t + \Delta t) - A_a(t)\, W_a(t) = -A_a(t) \frac{\Delta W}{\alpha} . \qquad (B5)$$

Adding and subtracting $A_a(t + \Delta t)\, W_a(t)$ from the left side of Eq. (B5) we obtain

$$A_a(t + \Delta t)\, [W_a(t + \Delta t) - W_a(t)] + W_a(t)\, [A_a(t + \Delta t) - A_a(t)] = -A_a(t) \frac{\Delta W}{\alpha} .$$

Dividing both sides by Δt and in the limit, as $\Delta t \to 0$:

$$\lim_{\Delta t \to 0} A_a(t + \Delta t) = A_a(t),$$

$$\lim_{\Delta t \to 0} \frac{W_a(t + \Delta t) - W_a(t)}{\Delta t} = \frac{dW_a(t)}{dt} = W_a'(t) ,$$

and

$$\lim_{\Delta t \to 0} \frac{A_a(t + \Delta t) - A_a(t)}{\Delta t} = \frac{dA_a(t)}{dt} = A_a'(t) ,$$

or

$$A_a(t)\, W_a'(t) + W_a(t)\, A_a'(t) = -A_a(t)\, (1/\alpha) \frac{dW}{dt} .$$

where $'$ denotes the derivative with respect to $\underline{t}$. Here dW is the mole quantity of hydrogen passing from the anode to the cathode chamber in time, $\underline{dt}$, and if we assume the process to go at a constant rate, then $dW/dt = K$. Also,

$$W_a(t) = W_{ao} - Kt;\ W_a'(t) = -K,$$

and

$$W_c(t) = W_{co} + Kt;\ W_c'(t) = K.$$

Thus, Eq. (B6) becomes

$$A_a(t)\ (-K) + W_a(t)\ A_a'(t) = -(K/\alpha)A_a(t),$$

$$A_a'(t) = [K - K/\alpha]\ A_a(t)\ [W_a(t)]^{-1},$$

and

$$A_a'(t)\ [A_a(t)]^{-1} = K\delta\ [W_a(t)]^{-1},$$

where $\delta = 1 - 1/\alpha$. Since $W_a(t) = W_{ao} - Kt$, then

$$\int_0^t \frac{A_a'(t)}{A_a(t)}\,dt = K\delta \int_0^t \frac{dt}{(W_{ao} - Kt)}.$$

Integrating, we have

$$\ln A_a(t)\Big|_0^t = K\delta\ (-1/K)\ \ln\ (W_{ao} - Kt)\Big|_0^t.$$

Noting that $A_a(0) = A_{ao}$, $A_a(t) = A_a$, and $W_{ao} - Kt = W_a(t) = W_a$, we have

$$\ln\left[\frac{A_a}{A_{ao}}\right] = \delta \ln\left[\frac{W_{ao}}{W_a}\right],$$

$$A_a/A_{ao} = (W_{ao}/W_a)^{\delta}, \text{ and}$$

$$A_a = A_{ao}\ (W_{ao}/W_a)^{\delta}. \tag{B7}$$

Noting that $\delta = 1 - 1/\alpha$ and solving for α explicitly, then

$$\alpha_a = 1 \Big/ \left[1 - \frac{\ln(A_a/A_{ao})}{\ln(W_{ao}/W_a)}\right], \tag{B7a}$$

where α_a denotes the bipolar separation factor as derived from the initial anode tritium balance at time, t.

ORNL-DWG 79-10630R

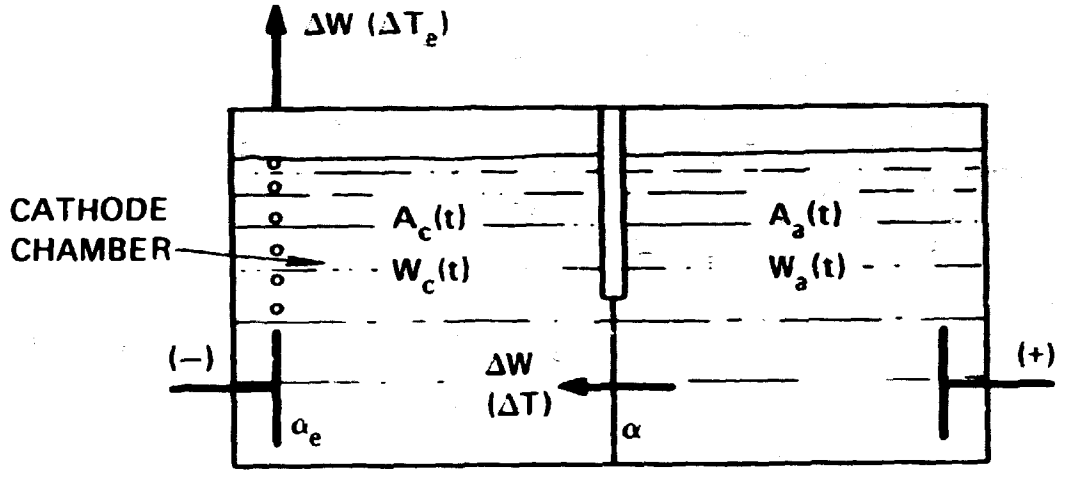

Figure B2. Variables associated with the cathode chamber of a cell having a single bipolar electrode:

$W_c(t)$ = moles of hydrogen in the cathode chamber at time t,

$A_c(t)$ = curies of tritium per mole of hydrogen at time t,

ΔT_e = incremental molar quantity of tritium exiting the cathode chamber,

α_e = terminal cathode separation factor.

Cathode Chamber Analysis

The change in tritium activity in the cathode chamber with time, for a cell having a single bipolar electrode, is influenced by two mass transfer processes. In one case hydrogen isotope atoms are introduced into the cathode chamber through the bipolar electrode. At the same time, an equivalent number of atoms are lost by the electrolytic production of isotope molecules at the terminal cathode. Both processes favor the transport of the lighter isotope. In effect the process at the terminal cathode enriches the cathode chamber electrolyte in tritium (or the heavier isotope). The rate of enrichment for this process is a function of the separation factor at the terminal cathode (α_e). The rate of change of tritium content in the cathode chamber is, simultaneously, affected by flow of tritium into the chamber via the bipolar electrode. The rate of tritium flow through the bipolar electrode is a function of the tritium content in the anode chamber, $A_a(t)$, and the bipolar separation factor, $\underline{\alpha}$.

The tritium balance in the cathode chamber at time $(t + \Delta t)$ is as follows:

(tritium at time $t + \Delta t$) = (tritium at time t) - (tritium in ΔW removed by cathode action) + (tritium in ΔW introduced through the bipolar electrode),

or

$$T_c(t + \Delta t) = T_c(t) - \Delta T_e + \Delta T. \qquad (B8)$$

In Eq. (B8), ΔT_e is a function of $A_c(t)$ and α_e, and ΔT is a function of $A_a(t)$ and α; thus, further substitution in Eq. (B8) will result in one

equation with two unknown separation factors, α and α_e. To eliminate this mathematical impass, we will assume that the cell is operated in a total cathode reflux mode (see Figure B3). In this mode of operation all cathode gas is burned, condensed, and returned to the cathode chamber (total reflux).

ORNL–DWG 79-10632R

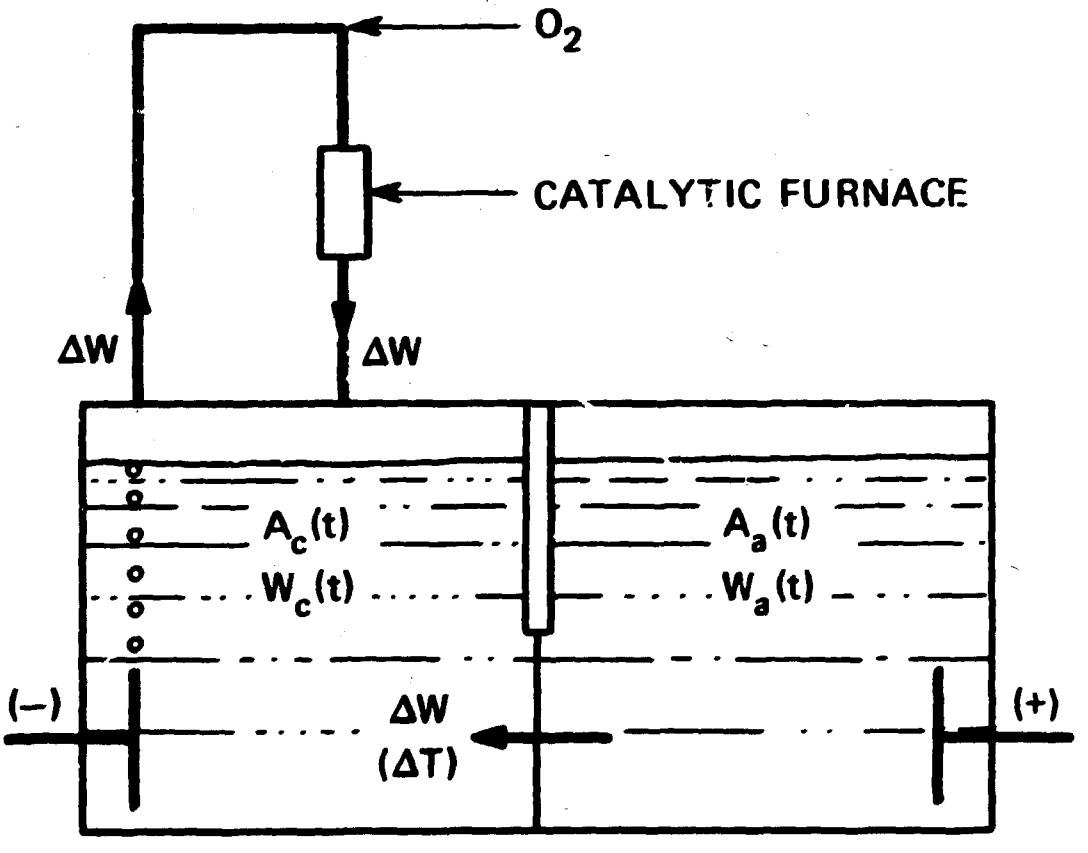

Figure B3. Schematic representation of a cell having a single bipolar electrode operating under a total reflux condition.

Under total reflux conditions the cathode tritium balance may be expressed as

$$T_c(t + \Delta t) = T_c(t) - \Delta T_e + \Delta T + \Delta T_e$$

$$T_c(t + \Delta t) = T_c(t) + \Delta T. \qquad (B9)$$

As with the anode tritium balance

$$\Delta T = A_a(t) \frac{\Delta W}{\alpha},$$

$$T_c(t + \Delta t) = A_c(t + \Delta t)\, W_c(t + \Delta t),$$

and

$$T_c(t) = A_c(t)\, W_c(t),$$

such that Eq. (B9) becomes

$$A_c(t + \Delta t)\, W_c(t + \Delta t) = A_c(t)\, W_c(t) + A_a(t) \frac{\Delta W}{\alpha}.$$

Dividing both sides of the equation by $W_c(t + \Delta t)$ and noting that $W_c(t + \Delta t) = W_c(t) + \Delta W$, we have

$$A_c(t + \Delta t) = \frac{A_c(t)\, W_c(t) + A_a(t) \frac{\Delta W}{\alpha}}{W_c(t) + \Delta W}.$$

Dividing numerator and denominator of the right side of the equation by $W_c(t)$ and simplifying, we have

$$A_c(t + \Delta t) = \left[A_c(t) + \frac{A_a(t)\ \Delta W}{\alpha W_c(t)} \right] \cdot \left[1 + \frac{\Delta W}{W_c(t)} \right]^{-1}. \qquad (B10)$$

Since $[1 + x]^{-1} = 1 - x + x^2 - \ldots\ldots$, therefore

$$[1 + \Delta W/W_c(t)]^{-1} = 1 - \Delta W/W_c(t) = [\Delta W/W_c(t)]^2 - \ldots\ldots .$$

Using this expression to expand Eq. (B10), we have

$$A_c(t + \Delta t) = A_c(t) + \frac{A_a(t)\ \Delta W}{\alpha W_c(t)} - \frac{A_c(t)\ \Delta W}{W_c(t)} - \frac{A_a(t)(\Delta W)^2}{\alpha\ [W_c(t)]^2} +$$

$$\frac{A_c(t)\ (\Delta W)^2}{[W_c(t)]^2} + \ldots .$$

Bringing $A_c(t)$ to the left hand side and dividing both sides of the equality by Δt, we have

$$\frac{A_c(t + \Delta t) - A_c(t)}{\Delta t} = \frac{A_a(t)}{\alpha W_c(t)} \cdot \frac{\Delta W}{\Delta t} - \frac{A_c(t)}{W_c(t)} \cdot \frac{\Delta W}{\Delta t} -$$

$$\frac{A_a(t)}{\alpha[W_c(t)]^2} \cdot \frac{(\Delta W)^2}{\Delta t} + \frac{A_c(t)}{[W_c(t)]^2} \cdot \frac{(\Delta W)^2}{\Delta t} + \ldots \qquad \text{(B11)}$$

In the limit as Δt approaches zero, we have

$$\lim_{\Delta t \to 0} \left[\frac{A_c(t + \Delta t) - A_c(t)}{\Delta t}\right] = \frac{dA_c(t)}{dt} = A_c'(t),$$

$$\lim_{\Delta t \to 0} \left[\frac{\Delta W}{\Delta t}\right] = \frac{dW}{dt} = K ,$$

and

$$\lim_{\Delta t \to 0} \left[\frac{(\Delta W)^2}{\Delta t}\right] = \lim_{\Delta t \to 0} \left[\frac{\Delta W}{\Delta t}\right] \cdot \lim_{\Delta t \to 0} (\Delta W) = \frac{dW}{dt} \cdot 0 = 0.$$

Since in the limit as Δt approaches zero, $(\Delta W)^p/\Delta t = 0$ for $p \geq 2$, Eq. (B11) reduces to the exact expression,

Noting that $W_a(t) = W_{ao} - Kt$, we have

$$K/\alpha \int_0^t A_a(t)\, dt = (K/\alpha) A_{ao} W_{ao}^{\delta} \int_0^t (W_{ao} - Kt)^{-\delta}\, dt$$

$$= (K/\alpha) A_{ao} W_{ao}^{\delta} \left[\frac{-1/K}{-\delta + 1}\right] (W_{ao} - Kt)^{-\delta + 1} \Bigg|_0^t$$

$$= \frac{1}{\alpha}\left[\frac{1}{\delta - 1}\right] A_{ao} W_{ao}^{\delta} \left[(W_{ao} - Kt)^{-\delta + 1} - W_{ao}^{-\delta + 1}\right] .$$

Substituting $\delta - 1 = -1/\alpha$ and $W_{ao} - Kt = W_a$, the expression becomes

$$K/\alpha \int_0^t A_a(t)\, dt = A_{ao}\left[W_{ao}\right]^{1 - \frac{1}{\alpha}} \left[W_{ao}^{1/\alpha} - W_a^{1/\alpha}\right] .$$

Substitution of these solutions into Eq. (B12) we have

$$A_c W_c - A_{co} W_{co} = A_{ao}\left[W_{ao}\right]^{1 - \frac{1}{\alpha}} \left[W_{ao}^{1/\alpha} - W_a^{1/\alpha}\right] .$$

Finally, solving for α explicitly,

$$\alpha = \frac{\ln W_a - \ln W_{ao}}{\ln[A_{ao}W_{ao} - A_c W_c + A_{co}W_{co}] - \ln A_{ao}W_{ao}}$$

$$A_c'(t) = K \left[\frac{A_a(t)}{\alpha} - A_c(t) \right] \Big/ W_c(t) .$$

Upon rearranging terms, the expression becomes

$$A_c'(t)\, W_c(t) + A_c(t)\, K = (K/\alpha)\, A_a(t), \text{ and}$$

noting that $K = W_c'(t)$, we have

$$A_c'(t)\, W_c(t) + A_c(t)\, W_c'(t) = (K/\alpha)\, A_a(t)$$

or

$$[A_c(t)\, W_c(t)]' = (K/\alpha)\, A_a(t) .$$

Integrating with respect to t, we have

$$\int_0^t [A_c(t)\, W_c(t)]'\, dt = K/\alpha \int_0^t A_a(t)dt . \qquad \text{(B12)}$$

Noting that $A_c(0)\, W_c(0) = A_{co}\, W_{co}$ and $A_c(t)\, W_c(t) = A_c W_c$, the solution of the left side of Eq. (B12) is as follows:

$$\int_0^t [A_c(t)\, W_c(t)]'\, dt = A_c W_c - A_{co}\, W_{co} .$$

Using the previously derived expression for $A_a(t)$ [Eq. (B7)], the solution of the right side of Eq. (B12) can be found, since

$$K/\alpha \int_0^t A_a(t)\, dt = K/\alpha \int_0^t A_{ao}\, W_{ao}^{\delta}\, [W_a(t)]^{-\delta}\, dt .$$

and noting that $A_i W_i = T_i$, then

$$\alpha_c = \frac{\ln W_a - \ln W_{ao}}{\ln [T_{ao} - T_c + T_{cc}] - \ln T_{ao}} \qquad \text{(B13)}$$

where α_c denotes bipolar separation factor derived from the cathode tritium balance.

Comparison of α_a and α_c

Although α_a and α_c were derived from analysis of different chambers of the bipolar cell and result in different expressions, α_a and α_c should be equal since both are a measure of the separation associated with the bipolar electrode. Using Eq. (B13) together with the fact that $T_i = A_i W_i$, we have

$$\alpha_c = \frac{\ln W_a - \ln W_{ao}}{\ln [A_{ao} W_{ao} - A_c W_c + A_{co} W_{co}] - \ln A_{ao} W_{ao}} . \qquad \text{(B14)}$$

Operating a bipolar cell in the total reflux mode results in the simple tritium balance

$$T_{ao} - T_a = T_c - T_{co}$$

or

$$A_{ao} W_{ao} - A_a W_a = A_c W_c - A_{co} W_{co} . \qquad \text{(B15)}$$

Equation (B15) simply states that the amount of tritium lost by the anode chamber is in turn gained by the cathode chamber. Solving for $A_a W_a$ in Eq. (B15) we have

$$A_a W_a = A_{ao} W_{ao} - A_c W_c + A_{co} W_{co} .$$

Substituting this result into Eq. (B14) results in the expression

$$\alpha_c = \frac{\ln W_a - \ln W_{ao}}{\ln[A_a W_a] - \ln[A_{ao} W_{ao}]} .$$

By manipulating logarithmic terms we have

$$\alpha_c = \frac{-\ln W_{ao}/W_a}{-\ln \frac{W_{ao}}{W_a} + \ln \frac{A_a}{A_{ao}}} .$$

Now dividing numerator and denominator by the term $-\ln (W_{ao}/W_a)$ we have

$$\alpha_c = 1 \Big/ \left[1 - \frac{\ln(A_a/A_{ao})}{\ln(W_{ao}/W_a)}\right] \qquad \text{(B16)}$$

Comparing Eq. (B16) with Eq. (B7a) we see that indeed

$$\alpha_c = \alpha_a .$$

APPENDIX C

MATHEMATICAL DESCRIPTION OF THE BIPOLAR ELECTROLYSIS SQUARE CASCADE

Steady-state cascade theory is concerned with the prediction of the stage requirements necessary for separation of a given isotope mixture into products of specified composition. From the theory, calculations should predict the number of stages needed for a desired separation, the local interstage flowrates and compositions, total separation for a given cascade, and other details necessary for cascade design.

The bipolar cascade is an inherently square cascade. Because of subtle differences between bipolar cascade design and conventional cascade modeling, it is necessary to derive the design equations specifically for bipolar electrolysis. A square bipolar cascade may be illustrated as shown in Figure C1.

ORNL-DWG 79-10634R

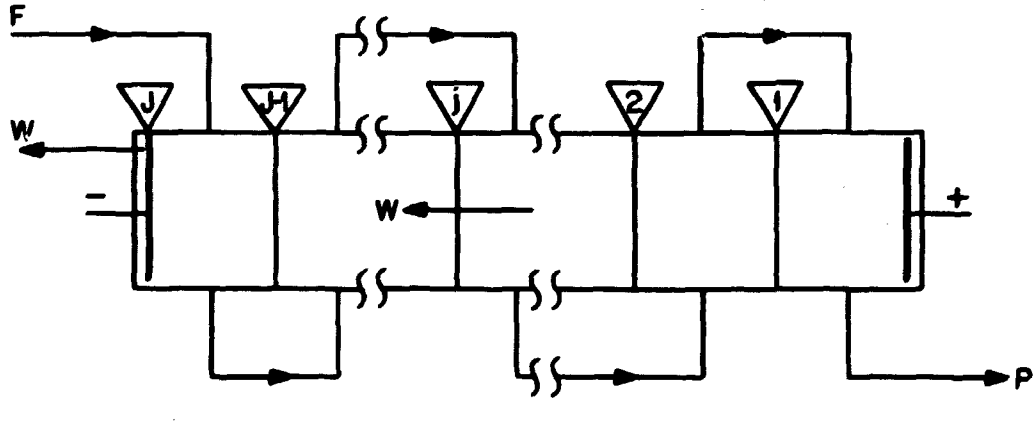

Figure C1. A Square Cascade Bipolar Electrolytic System

Transformation of Fig. C1 into a more conventional cascade diagram is illustrated in Fig. C2.

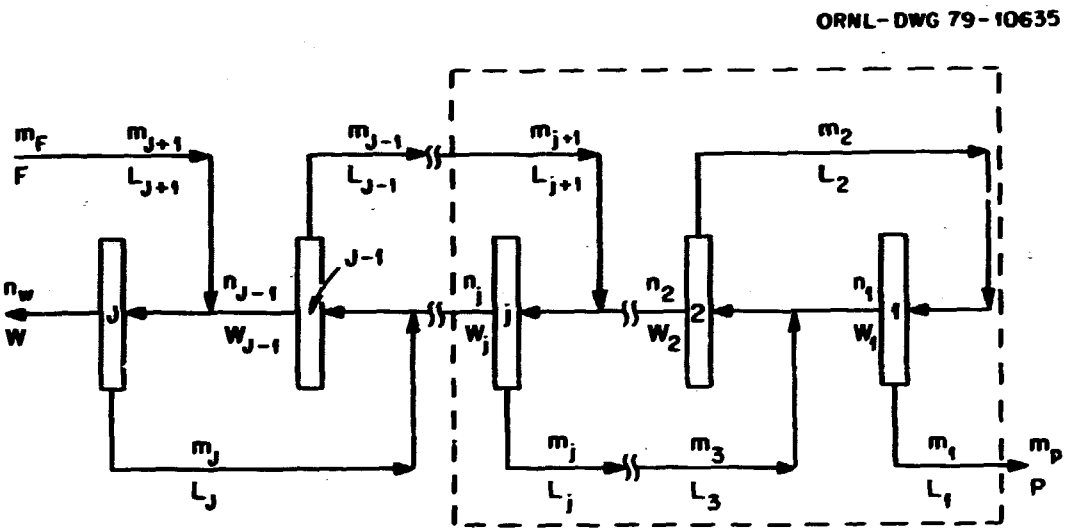

Figure C2. Bipolar Electrolysis Cascade and Flow Scheme

Let L_j denote the molar flow rate of the stream enriched in the heavier isotope leaving the j'th stage, and let m_j denote the composition (mole fraction) of the L_j stream. Let W_j denote the molar flow rate of the stream depleted in the heavier isotope leaving the j'th stage, and let n_j denote the composition (mole fraction) of the W_j stream. Performing a material balance (for the heavy isotope) at the product end of the cascade (stage 1) and stage j,

$$L_{j+1}\, m_{j+1} = W_j\, n_j + P\, m_p \,. \qquad (C1)$$

A molar flow rate balance around stage 1 gives

$$L_2 = W_1 + P. \tag{C2}$$

For a square cascade (i.e., a square section of a bipolar cascade) we have

$$W_1 = W_2 = \ldots W_J = W, \text{ and}$$

therefore, Eq. (C2) becomes

$$L_2 = W + P. \tag{C3}$$

Now from a molar flow rate balance around the entire cascade we have

$$F = W + P, \tag{C4}$$

and comparing Eq. (C3) and (C4), it is seen that

$$L_2 = F.$$

Similar analysis around stages 1 and 2 yields

$$L_3 = F,$$

and repeating the analysis we find that

$$L_2 = L_3 = \ldots L_{J+1} = F.$$

Therefore, Eq. (C1) becomes

$$F\, m_{j+1} = W\, n_j + P\, m_p,$$

or

$$m_{j+1} = (W/F) n_j + (P/F) m_p. \tag{C5}$$

Letting $\rho \equiv (P/F)$ and using Eq. (C4) we see that

$$1 = (W/F) + (P/F) \longrightarrow 1 = (W/F) + \rho$$

or

$$(W/F) = 1 - \rho.$$

Substituting these results into Eq. (C5) we have

$$m_{j+1} = (1 - \rho)\, n_j + \rho m_p. \tag{C6}$$

By rewriting Eq. (C6) for m_{j+2},

$$m_{j+2} = (1-\rho)\, n_{j+1} + \rho m_p \qquad \text{(C7)}$$

and subtracting Eq. (C7) from (C6) then yields

$$m_{j+1} - m_{j+2} = (1-\rho)\,(n_j - n_{j+1}). \qquad \text{(C8)}$$

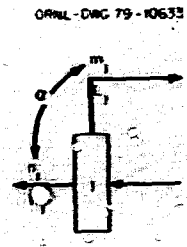

Figure C3. Single Stage Flow Scheme

Referring to Fig. C3, the separation factor for any stage is defined as

$$\alpha = \frac{m_j(1-n_j)}{n_j(1-m_j)}.$$

For small concentrations of the heavier isotope, (i.e., <0.01 mole fraction) the quantity $(1-n_j)/(1-m_j) \cong 1$. Using this approximation, the separation factor may be written as

$$\alpha \cong \frac{m_j}{n_j}. \qquad \text{(C9)}$$

From Eq. (C9)

$$n_j = (1/\alpha)\, m_j \qquad \text{and} \qquad n_{j+1} = (1/\alpha)\, m_{j+1},$$

and using these results in Eq. (C8) we have

$$m_{j+1} - m_{j+2} = \frac{(1-\rho)}{\alpha}\,(m_j - m_{j+1}). \qquad \text{(C10)}$$

Letting

$$\Omega = \frac{\alpha}{(1 - \Omega)} \longrightarrow (1/\Omega) = \frac{1 - \rho}{\alpha}, \text{ the}$$

Eq. (C10) becomes

$$m_{j+1} - m_{j+2} = (1/\Omega)\,(m_j - m_{j+1}),$$

upon rearranging terms

$$m_{j+2} - m_{j+1} = (1/\Omega)\,(m_{j+1} - m_j) \qquad \text{(C11)}$$

Now let $j = 2,1, \ldots J$ and noting that $j = 1$, $m_j = m_1 \equiv m_p$, Eq. (C11) generates the following array of equations:

$$m_2 - m_p = (m_2 - m_p)$$

$$(j = 1); \quad m_3 - m_2 = (1/\Omega)\,(m_2 - m_1) = (1/\Omega)\,(m_2 - m_p)$$

$$(j = 2); \quad m_4 - m_3 = (1/\Omega)\,(m_3 - m_2) = (1/\Omega)^2\,(m_2 - m_p)$$

$$(j = 3); \quad m_5 - m_4 = (1/\Omega)\,(m_4 - m_3) = (1/\Omega)^3\,(m_2 - m_p)$$

$$\vdots$$

$$(j = J) \quad m_{J+2} - m_{J+1} = (1/\Omega)\,(m_{J+1} - m_J) = (1/\Omega)^J\,(m_2 - m_p).$$

With the identity $(m_2 - m_p) = (m_2 - m_p)$ added at the top of the left and right columns, the sum of all the equations yields,

$$m_{J+2} - m_p = (1 + 1/\Omega + 1/\Omega^2 + \ldots + 1/\Omega^J)\,(m_2 - m_p) \qquad \text{(C12)}$$

Using Equation (C6) and letting $j = 1$, we have

$$m_2 = (1 - \rho)\,n_1 + \rho m_p \qquad \text{(C13)}$$

Noting from Equation (C9) that $n_1 = (1/\alpha)\,m_1 = (1/\alpha)\,m_p$, Eq. (C13) becomes

$$m_2 = \left(\frac{1}{\alpha} - \rho\right) m_p + \rho m_p = (1/\Omega)\,m_p + \rho m_p. \qquad \text{(C14)}$$

Subtracting m_p from both sides of Equation (C14),

$$m_2 - m_p = \left[\rho + (1/\Omega) - 1\right] m_p. \qquad \text{(C15)}$$

Substituting Eq. (C15) into Eq. (C12),

$$m_{J+2} - m_p = (1 + 1/\Omega + 1/\Omega^2 + \ldots + 1/\Omega^J)\,[\rho + (1/\Omega) - 1]\, m_p. \qquad \text{(C16)}$$

Now we note that

$$1 + 1/\Omega + 1/\Omega^2 + \ldots + 1/\Omega^J = \frac{1 - 1/\Omega^{J+1}}{1 - 1/\Omega},$$

and Eq. (C16) then becomes

$$m_{J+2} - m_p = \frac{1 - 1/\Omega^{J+1}}{1 - 1/\Omega}\,[\rho + (1/\Omega) - 1]\, m_p. \qquad \text{(C17)}$$

Expressing Eq. (C17) in terms of J + 1, rather than J + 2, and rearranging terms

$$m_{J+1} = m_p \frac{[\rho + (1/\Omega) - 1]\,(1 - 1/\Omega^J) + 1 - 1/\Omega}{1 - 1/\Omega}$$

or

$$m_{J+1} = m_p \left[1/\Omega^J + \rho\,\frac{(1 - 1/\Omega^J)}{1 - 1/\Omega}\right]. \qquad \text{(C18)}$$

Comparing the nomenclature of Eq. (C18) with the cascade shown in Fig. C2, see that m_{J+1} is m_F, the mole fraction of the feed to the cascade. Therefore, Eq. (C18) becomes

$$m_F = m_p \left[1/\Omega^J + \rho\,\frac{(1 - 1/\Omega^J)}{(1 - 1/\Omega)}\right]. \qquad \text{(C19)}$$

Converting to more conventional variables,

$$\hat{\alpha} = \frac{\alpha}{1-\rho} = \alpha \frac{1}{1-\rho} = \alpha \frac{1}{1-P/F}$$

and letting

$$\phi \equiv \frac{1}{1-P/F} ,$$

then

$$\Omega = \alpha\phi ,$$

and Eq. (C19) becomes

$$m_F = \beta\, m_p$$

with

$$\beta = (1/\alpha\phi)^J + \frac{P}{F}\left(\frac{1-(1/\alpha\phi)^J}{1-(1/\alpha\phi)}\right), \qquad \text{(C20)}$$

where

m_F = Mole fraction of the heavier isotope in the feed stream,

m_p = Mole fraction of the heavier isotope in the product stream,

$\phi = \frac{1}{1-P/F}$,

α = Single stage bipolar separation factor,

P = Molar flow rate of product and has the units of total moles of hydrogen[1]/unit time,

F = Molar flow rate of feed; has the units of total moles of hydrogen/unit time, and

J = Total number of separation stages in a square section.

---

[1]Total moles of hydrogen = the total molar flow rate of any two hydrogen pairs as $H_2 + T_2$, $H_2 + D_2$ or $D_2 + T_2$